

A New Isostatic Residual Gravity Map of the Conterminous United States With a Discussion on the Significance of Isostatic Residual Anomalies

R. W. SIMPSON, R. C. JACHENS, AND R. J. BLAKELY

U.S. Geological Survey, Menlo Park, California

R. W. SALTUS

U.S. Geological Survey, Denver, Colorado

To display more clearly the gravity anomalies caused by geologic bodies in the upper parts of the crust, a new colored isostatic residual gravity map of the conterminous United States has been prepared using the gravity data set compiled for the Gravity Anomaly Map of the United States (Society of Exploration Geophysicists, 1982). The new isostatic residual gravity map is based on an Airy-Heiskanen model of local compensation, in which the surface load requiring compensation is defined by 5-min topographic and bathymetric data sets. A colored first-vertical-derivative map of isostatic residual gravity further enhances the short-wavelength anomalies produced by bodies at or near the surface and emphasizes the regional fabrics and trends in the gravity field. For the purpose of displaying gravity anomalies caused by shallow bodies of geologic significance, the nature of the isostatic model and the values of its parameters are of lesser importance than the application of an isostatic correction of some sort. Most isostatic models result in residual gravity maps that appear nearly identical in their main patterns and features. Anomalies on isostatic residual gravity maps should not be casually interpreted in terms of "undercompensation" or "overcompensation" because large-amplitude anomalies can be produced by crustal bodies in complete local isostatic equilibrium. Many isostatic residual gravity anomalies less than several hundred kilometers wide can be related to known geologic bodies. We present here a classification scheme that attempts to categorize such anomalies on the basis of tectonic environment. In general, highs correlate with intruded or accreted mafic material or with upthrust crustal sections, whereas lows occur over low-density sedimentary or volcanic sections, felsic intrusive bodies, or down-warped crustal sections. Although some longer-wavelength anomalies, such as the broad gravity high centered over Montana, could be manifestations of density contrasts deep in the mantle, many such anomalies can also be modeled by geologically reasonable density contrasts that are isostatically compensated and confined to depths of less than several hundred kilometers, so that their source bodies need not be deep. The fact that certain of these broader anomalies have well-defined boundaries which correlate with near-surface geologic features increases the likelihood that their sources lie entirely within the lithosphere. If so, then the density contrasts required to explain the gravity data imply fundamental anomalies in chemical composition or thermal state for the crustal and upper mantle columns under these regions. We have investigated spectral analysis as a method to quantitatively characterize regional anomaly patterns. Contoured plots of normalized amplitude spectra were prepared for various areas of the isostatic residual gravity field of the United States. These Fourier domain representations show characteristic patterns that can be interpreted in terms of the trends and wavelengths of anomalies and may help to more objectively distinguish geologic basements with different origins or tectonic histories.

INTRODUCTION

Hayford and Bowie [1912] published the first isostatic gravity anomaly map of the United States in color (see Table 1). This map, showing "lines of equal anomaly for [the] new method of reduction," was based on 89 pendulum gravity observations collected at various sites around the country. Remarkably, the 89 observations sampled nearly every major anomaly in the isostatic gravity field of the conterminous United States.

A new version of the isostatic gravity map (Plate 1) has recently become possible with the compilation of a gravity data base, containing 1 million observations on land and 0.8 million at sea, that was used to prepare the Gravity Anomaly Map of the United States [*Society of Exploration Geophysicists*, 1982]. (Plate 1 can be found in the separate color section in this issue.) The preparation of this new isostatic map was

greatly simplified by two other recent developments: Computers and digital data bases have removed the enormous burden of calculation, and the advent of computer-driven color plotters has made it possible to quickly display the data in unprecedented detail.

Since the time that *Airy* [1855] and *Pratt* [1855] introduced the concept of crustal balance, and *Dutton* [1889] proposed the term isostasy to encompass it, much effort has been directed toward establishing the existence of isostatic equilibrium over most of the earth's surface, toward understanding the nature of the isostatic mechanism, and toward determining the most appropriate models for isostatic compensation within various geologic and tectonic provinces. *Daly* [1940] summarized early work along these lines in the United States; examples of more recent studies were presented by *Dorman and Lewis* [1970, 1972], *Lewis and Dorman* [1970], *McNutt* [1980], and *Mörner* [1980].

A second research direction has focused on the ability of isostatic gravity maps, with all topography-related anomalies removed to first approximation, to enhance information about density contrasts within the upper crust and to aid in the

This paper is not subject to U.S. copyright. Published in 1986 by the American Geophysical Union.

Paper number 5B5811.

TABLE 1. Isostatic Gravity Maps of the United States

Observations	Scale	Reference
89	1:7,000,000	Hayford and Bowie [1912]
124	1:7,000,000	Bowie [1912] and Gilbert [1913]
219	1:7,000,000	Bowie [1917]
296	1:22,000,000	Bowie [1924]
~ 1,000	1:14,600,000	Woollard [1936]
~ 200,000	1:14,200,000	Woollard [1966]
80,000	1:41,300,000	Lewis and Dorman [1970]
unknown	1:20,300,000	McNutt [1980]
1,800,000	1:2,500,000	Jachens et al. [1986a]
1,800,000	1:7,500,000	Simpson et al. [1986]

extrapolation of mapped surface geology into the subsurface. Gilbert [1913] recognized the utility of isostatic gravity maps for outlining density distributions associated with geologic bodies, and he clearly understood the problems and uncertainties associated with the interpretation of isostatic anomalies. Woollard [1936, 1962, 1966, 1968] spent much of his career investigating the relations of isostatic gravity anomalies to mapped geologic features and to crustal parameters determined from seismic experiments. Rabinowitz and LaBrecque

[1977] and Karner and Watts [1982] used isostatic anomalies to illuminate the evolution of the ocean-continent boundary.

Our interest in preparing a new isostatic gravity map has been along these latter lines. We believe that isostatic residual gravity maps reveal more clearly than most gravity maps the density distributions within the crust that are of interest in many kinds of geologic and tectonic analyses. For such analyses, application of an isostatic correction of some sort is more important than the exact nature of the isostatic model or the values of its parameters; most isostatic residual gravity maps, regardless of model, appear quite similar in their main patterns and features. Contoured and colored versions of the new isostatic residual gravity map are being published at several scales [Jachens et al., 1986b; Simpson et al., 1986] to facilitate comparisons with existing geologic, tectonic, basement, and aeromagnetic maps.

In the discussion that follows, isostatic regional refers to the gravity field caused by the isostatic compensating masses, and isostatic residual refers to gravity anomalies that remain after the isostatic regional field has been subtracted from the Bouguer gravity; that is, after the isostatic correction has been applied. Isostatic residual gravity maps have been called

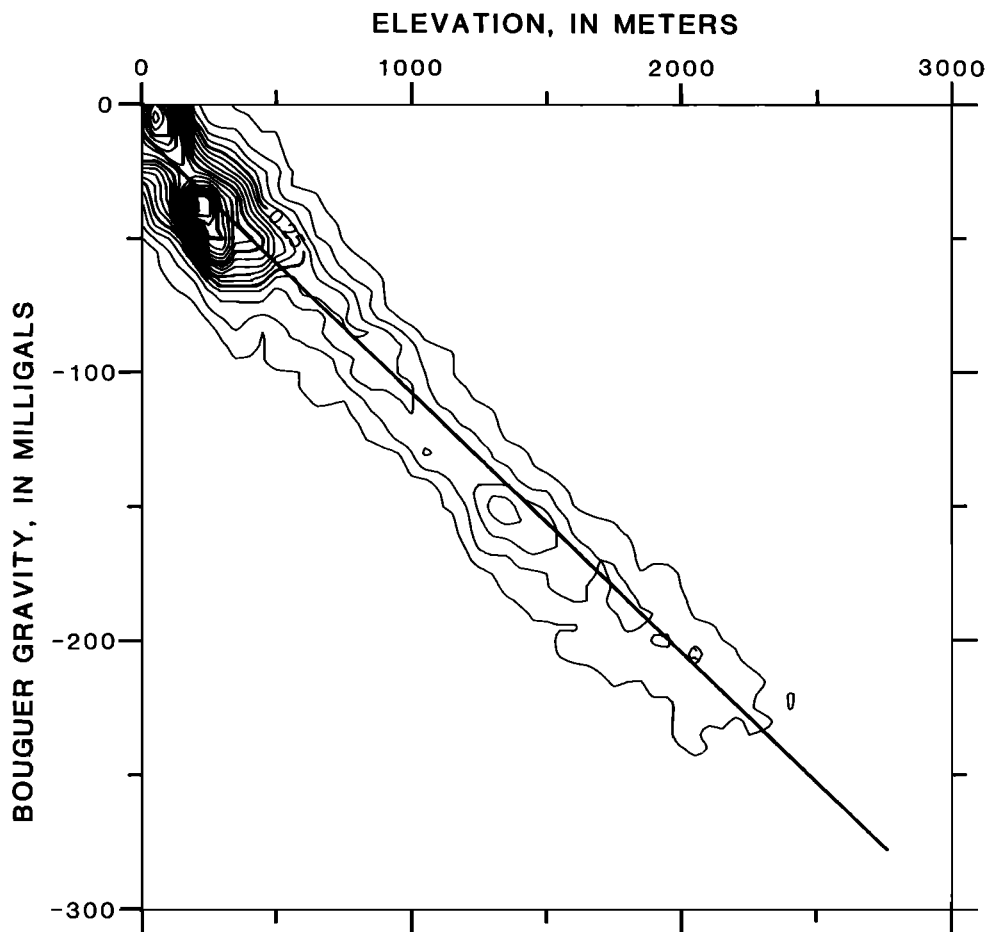


Fig. 1. Inverse correlation of onland Bouguer gravity anomaly values with elevation for the conterminous United States. Bouguer gravity and topography grids described in the text were sampled at 20-km intervals to obtain the values for this two-dimensional histogram. The numbers of grid points falling into 5-mGal-tall by 50-m-wide cells were counted, these numbers were normalized by dividing by the largest number, and the results were contoured at 0.05 (5%) intervals after a small amount of smoothing. Closed high at about 250 m, which falls slightly below the main trend, is caused by broad areas of low Bouguer value in the midcontinent, which can also be seen on the isostatic residual map (Plate 1). A regression line $y' = a + bx$ is shown, for which $a = -11.5$ and $b = -0.0942$; standard error of estimate, 24.0; correlation coefficient, -0.942 .

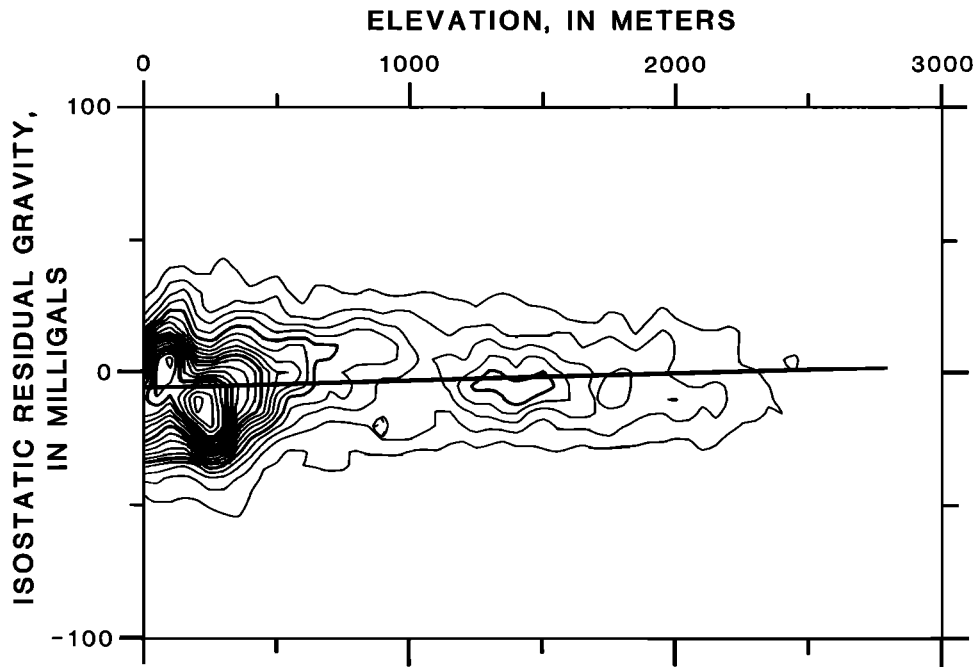


Fig. 2. Isostatic residual gravity values versus elevations for the conterminous United States. Constructed as in Figure 1. A regression line $y' = a + bx$ is shown, for which $a = -6.7$ and $b = 0.0039$; standard error of estimate, 18.5; correlation coefficient, 0.148.

simply isostatic gravity maps in the past. We use the word residual partly to be more explicit and partly in the hope that its unfamiliar ring will assist the reader to avoid some of the pitfalls that arise in the interpretation of isostatic maps. One of the commonest pitfalls is the tendency to interpret all isostatic residual gravity anomalies in terms of “undercompensation” or “overcompensation,” a tendency that is generally unproductive for reasons to be discussed in a later section.

THE ISOSTATIC CORRECTION

Over much of the earth's surface, the longer wavelengths of the Bouguer gravity field correlate inversely with the longer wavelengths of topography (Figure 1). For the conterminous United States, this inverse correlation is readily seen on wavelength-filtered maps of Bouguer gravity, and topography for which wavelengths shorter than 250 km have been suppressed [Simpson *et al.*, 1982]. The principle of isostasy offers an explanation for this inverse correlation: loads on the earth's surface produced by topographic features are supported at depth by deficiencies in mass, as if the earth's crust were floating on a denser substratum [Airy, 1855; Dutton, 1889; Woollard, 1966; Heiskanen and Moritz, 1967]. These deficiencies in mass under topographic loads are commonly called compensating masses or roots. The Bouguer reduction process removes, for the most part, the gravitational attraction of topographic masses down to sea level and replaces the water in lakes and oceans with material of a more nearly average density (generally, 2.67 g/cm^3). Thus, in mountainous areas the compensating masses, which have not been accounted for in the Bouguer reduction process, manifest themselves as broad Bouguer gravity anomaly lows. In contrast, oceanic crustal columns have a negative load at the surface because water is less dense than rock; to maintain isostatic balance, this density difference requires the existence at depth of a compensat-

ing mass excess or antiroot. Thus the compensating masses in oceanic areas produce broad Bouguer anomaly highs.

The isostatic reduction attempts to remove the attraction of the compensating masses. Figure 2 shows the lack of correspondence between gravity anomaly values and topographic elevation in the conterminous United States after an isostatic correction has been applied. Bouguer gravity anomaly values spanning a range of more than 300 mGal have been reduced to isostatic residual gravity values spanning about 100 mGal (Figure 3).

Most isostatic corrections are based on simple models for the geometry of the compensating masses, and such models are of necessity highly idealized representations of the real-

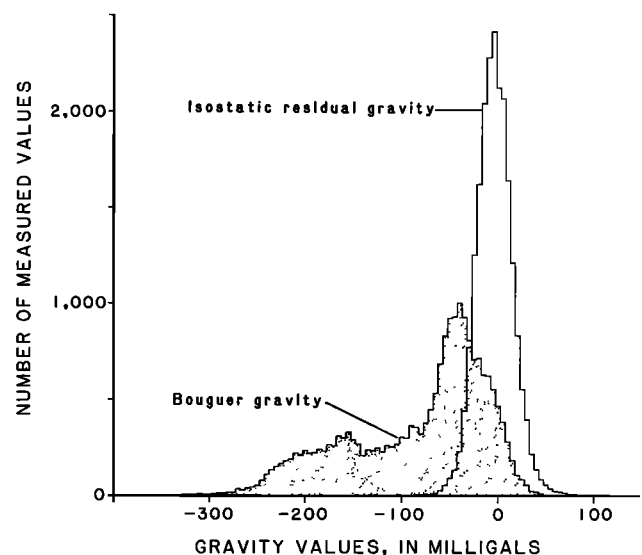


Fig. 3. Comparison of the distribution of onland Bouguer gravity values with the distribution of isostatic residual gravity values for the conterminous United States.

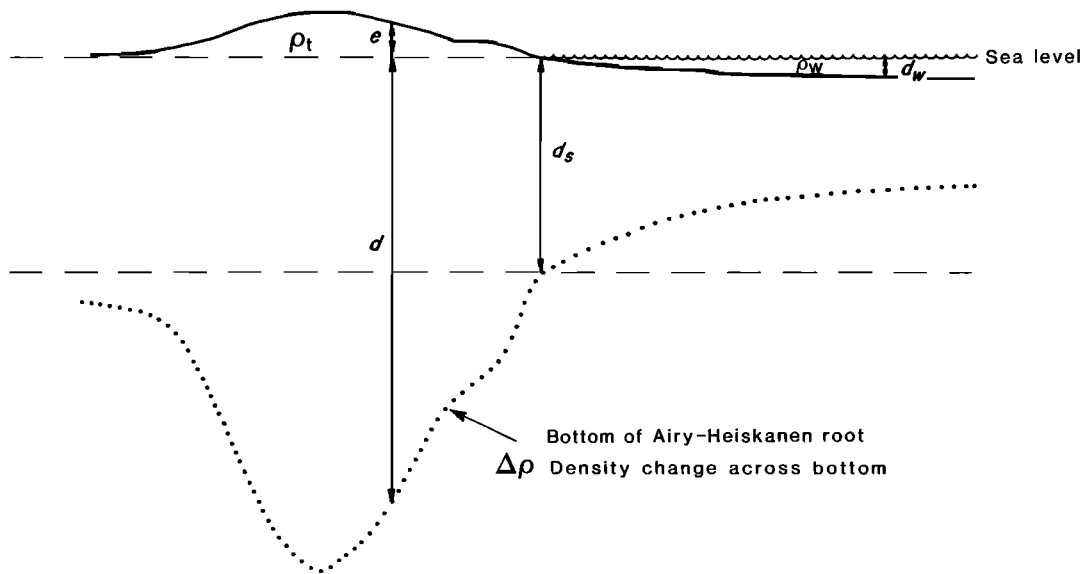


Fig. 4. Geometry of compensating masses in Airy-Heiskanen local compensation model: e , elevation of topographic surface above sea level; d , depth to bottom of root; d_s , depth to bottom of root for sea level elevation; ρ_t , density of topography; d_w , depth of water in ocean areas; ρ_w , density of water; $\Delta\rho$, density contrast at depth across bottom of root.

world geometries. It would be desirable to incorporate additional geophysical data into the construction of an isostatic model, and interesting integrations of gravity and seismic data are being tried in areas where good data on seismic velocities and depths to the Mohorovičić (M) discontinuity are available [e.g., *Sprenke and Kanasevich*, 1982; *Gettings et al.*, 1986]. It appears to us, however, that neither the quality nor the quantity of such data yet permits such an application on a continent-wide scale. Various isostatic models and values for their parameters have been tried over the years, including statistical approaches that infer the best isostatic response function from the data themselves [e.g., *Neidell*, 1963; *Dorman and Lewis*, 1970] and models that incorporate the strength of the crust and its role in distributing compensation laterally [e.g., *McNutt*, 1983; *Stephenson and Lambeck*, 1985]. No single model or response function is likely to be appropriate for an entire continental area, given the typical diversity of tectonic environments on any given continent. Almost all reasonable isostatic models produce similar results, however, because the total compensating mass for all models should be the same and the compensating masses generally are sufficiently deep that their gravitational effects observed at the earth's surface are smoothed by distance. Thus the differences in the isostatic corrections predicted by various models tend to be a small percentage of the total correction [*Jachens and Griscom*, 1985; *Saltus*, 1984]. For the removal of topography-induced regionals and the enhancement of gravity anomalies related to shallow geologic features, an isostatic correction based on even a simple model is ordinarily preferable to the extraction of a regional by such techniques as empirical smoothing, polynomial fitting, or wavelength filtering because the isostatic regional is designed to remove an observed correlation between Bouguer values and topography. These alternate methods may still be needed after the isostatic correction has been applied to separate anomalies not related to topographic loads.

Many isostatic models yield regionals that can be approximated, to first order, by spreading the compensating masses on a two-dimensional sheet at some depth d related to the

depth of compensation. The isostatic regional field produced by this simple mass distribution is proportional to the field obtained by upward continuation of the topographic elevations to a height d , as if they defined a potential field. (See *McNutt* [1980] for the equation for linear Airy compensation.) Thus isostatic regionals are smoothed versions of the topography. This observation explains why other approaches to the removal of isostasy-induced anomalies, such as the Faye anomaly [*Putnam*, 1894, 1895; *Mabey*, 1966], the Graaff-Hunter reduction [*Graaff-Hunter*, 1958], and the residual Bouguer correction method [*Aiken*, 1976; *Aiken et al.*, 1981], produce results very similar to an isostatic correction. All these methods apply a correction based on averaged topography rather than on an isostatic model, and the averaging process suppresses short wavelengths in the topography, as does the upward continuation filter. Distributing the compensating masses [*Vening Meinesz*, 1939; *Banks et al.*, 1977; *McNutt*, 1980] rather than having them entirely local (that is, directly under the load) can also have a smoothing effect not unlike additional upward continuation of the topographic load. These considerations explain why it is so difficult to determine the actual isostatic mechanism operating in the earth from gravity evidence alone, and why most reasonable isostatic models give results that are so generally similar.

One weakness to our approach in this report is that we have ignored crustal and lithospheric strength: the possibility of distributing compensation and of supporting loads regionally by elastic flexure of the lithosphere. *Banks et al.* [1977] demonstrated that to a high degree of probability, the isostatic response function for the conterminous United States taken as a whole is best explained by a regional compensation mechanism. By examining the response functions for the western and eastern halves of the country separately, *McNutt* [1980] concluded that compensation in the west was essentially local in nature, whereas compensation in the east was required to be nonlocal. We could have chosen elastic parameters and used a regional compensation model to prepare Plate 1, but for our purposes we did not think that the result would appear different enough to warrant the additional as-

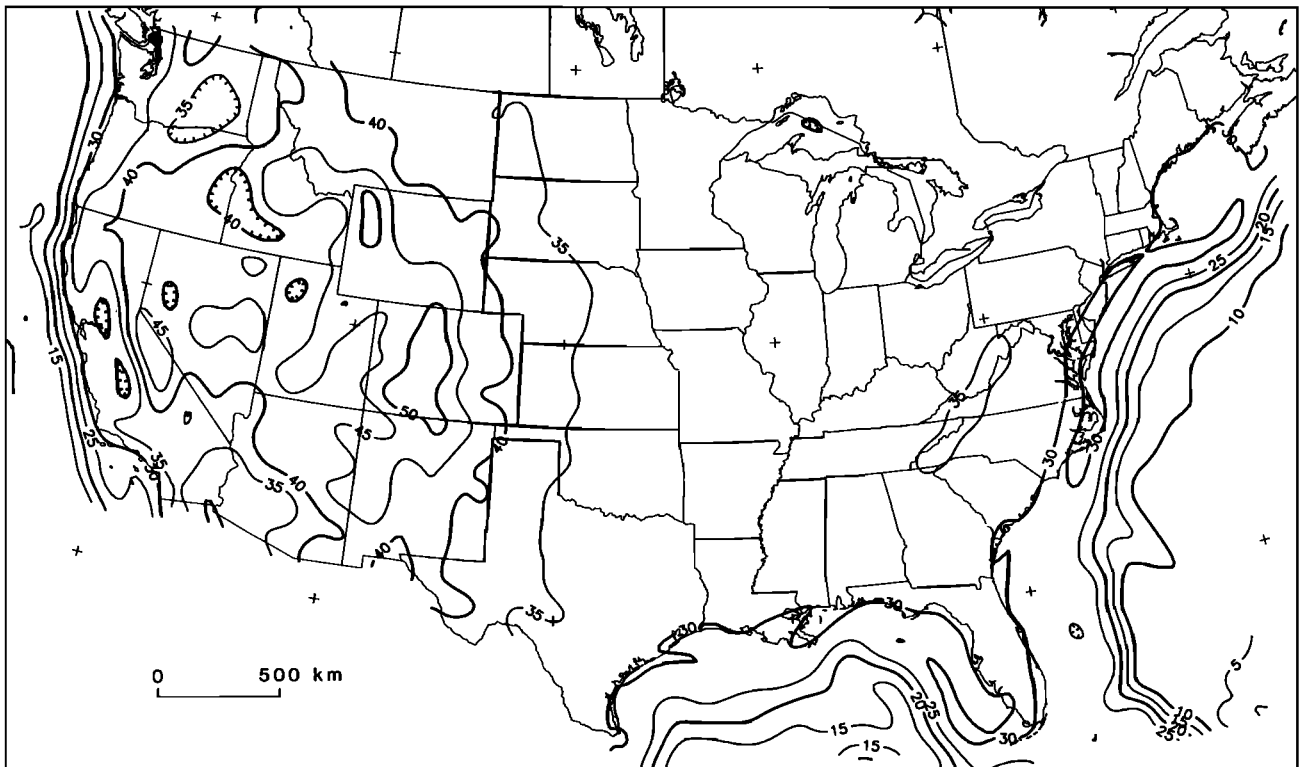


Fig. 5. Depth to bottom of Airy-Heiskanen root for $\rho_t = 2.67 \text{ g/cm}^3$, $\Delta\rho = 0.35 \text{ g/cm}^3$, and $d_s = 30 \text{ km}$. Contour interval, 5 km. Map has been smoothed by low-pass wavelength filtering, with a cutoff at 200 km in the Fourier transform domain. Hachures on closed contours point toward smaller depth values.

sumptions. Moreover, a single set of elastic parameters does not seem able to do justice to the entire country.

PREPARATION OF THE ISOSTATIC RESIDUAL GRAVITY MAP

Gravity values for the new map came from the gridded data set described by *Godson and Scheibe* [1982], which was assembled to prepare a gravity anomaly map of the United States [*Society of Exploration Geophysicists*, 1982]. This grid has a 4- by 4-km interval and contains Bouguer gravity values onshore and free air values offshore. The distribution of the 1×10^6 gravity observations on land and 0.8×10^6 at sea that were used to make the grid is shown as an inset on the *Society of Exploration Geophysicists* [1982] map. For onshore areas, approximately 95% of all 5- by 5-min cells have at least one gravity observation available. Additional information on the construction of this grid was given by *O'Hara and Lyons* [1983].

Bathymetric and topographic data sets were obtained from the U.S. National Oceanic and Atmospheric Administration (NOAA) Data Center. Details on the process of combining these 5-min data sets were presented by *Simpson et al.* [1983a, b]; the combined data sets are shown in Plate 2. Tests suggest that 5-min topographic data adequately define the geometry of the root for regional scale maps, although 3-min data are more suitable for smaller scales.

We chose to use an Airy-Heiskanen model with local compensation [*Heiskanen and Moritz*, 1967]. This model requires a choice of values for three parameters: a depth of compensation for sea level elevations d_s , a density contrast across the bottom of the root $\Delta\rho$, and a density of the topographic load ρ_t (Figure 4). These parameters determine the depth d to the bottom of the root under land areas by the relation

$$d = d_s + e \left(\frac{\rho_t}{\Delta\rho} \right) \quad (1)$$

where e is the elevation of the topographic surface. The weight of the water in the Great Lakes was added to the topographic load in the calculation of the root.

In the Airy-Heiskanen scheme, oceanic crustal columns with water depth d_w (taken to be positive here) have a negative load (weight deficiency) at the top caused by the presence of water of density ρ_w rather than rock [*Heiskanen and Moritz*, 1967]. Negative compensation is provided by an antiroot of denser material that has its top at a depth

$$d = d_s - d_w \left(\frac{\rho_t - \rho_w}{\Delta\rho} \right) \quad (2)$$

In many published figures depicting the geometry of the Airy-Heiskanen compensation model it appears that the entire crustal column above the bottom of the root must have the same density as the topography. No such restriction, however, is required by the equations: the density of the model crust below sea level may change as a function of depth, provided only that the superposed changes with depth are horizontally uniform and the density contrast across the bottom of the root is constant regardless of depth. The density of the topography serves to define the weight of the surface load; the model does not require that this density extend into the subsurface.

For the Airy-Heiskanen parameters we chose a depth to the bottom of the root of 30.0 km for sea level elevations, a density contrast across the root of 0.35 g/cm^3 , and a topographic density of 2.67 g/cm^3 . These parameters give a root geometry (Figure 5) that over large parts of the conterminous United States is close to the geometry of the M discontinuity as deter-

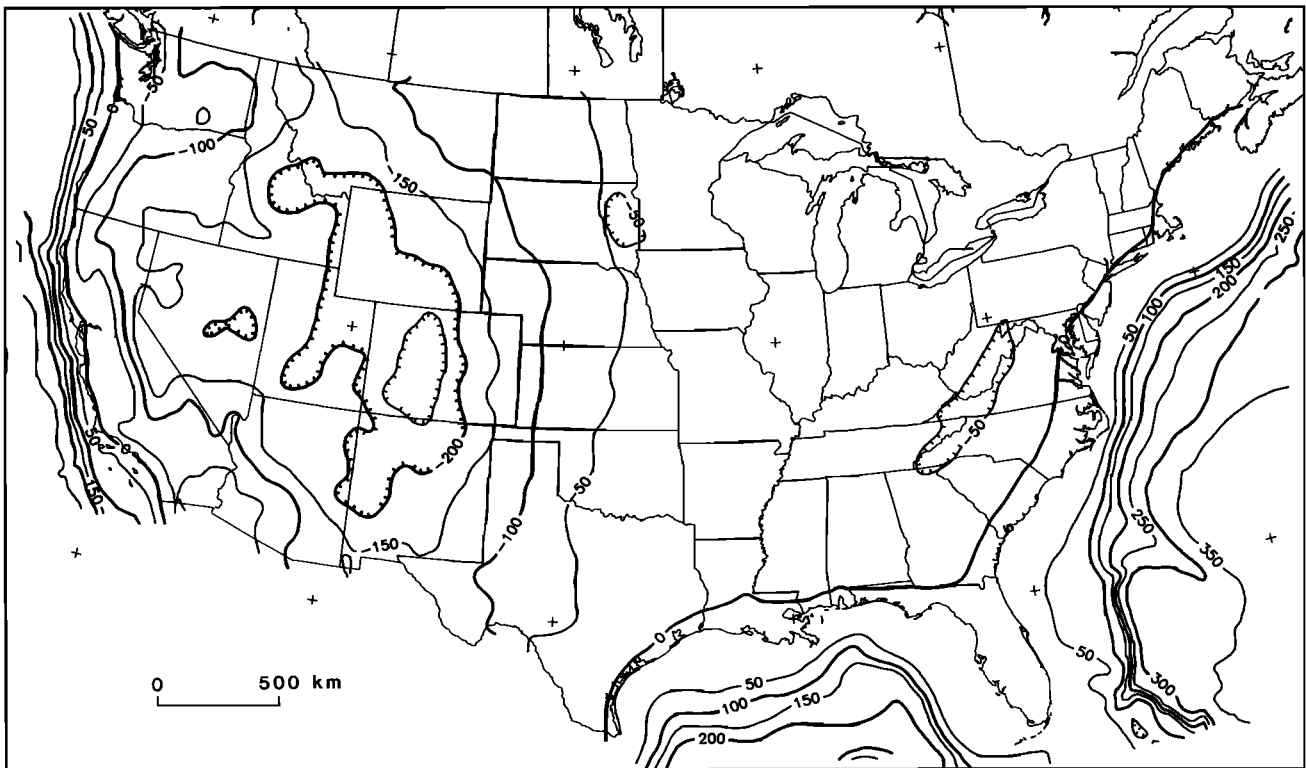


Fig. 6. Isostatic regional gravity field in milliGals at sea level. Contour interval 50 mGal. This is the gravitational attraction of the compensating masses (roots) in the Airy-Heiskanen model, with the same parameters as in Figure 5. This attraction, after upward continuation to the surface elevation, is subtracted from the Bouguer gravity field as an isostatic correction to give the isostatic residual gravity shown in Plate 1. Hachures on closed contours point toward lower regional values.

mined by seismic refraction experiments [Woollard, 1968, equation (1)]. The M discontinuity is an appropriate depth for the bottom of an Airy root (for want of better information) because it is a major velocity discontinuity that is probably accompanied by an important density discontinuity. However, especially in the western United States, major discrepancies exist between the calculated depth to the bottom of the Airy-Heiskanen root and the depth to the seismically determined M discontinuity [Allenby and Schnetzer, 1983]. Clearly, no simple isostatic model can possibly provide an accurate description of the geometries of the compensating masses for an entire continental area.

The attraction of the Airy-Heiskanen root at a point on the earth's surface (Figure 6) was calculated in two steps. The attraction on a flat earth out to a distance of 166.7 km was calculated by using a program [Simpson *et al.*, 1983a] based on the fast Fourier transform algorithm developed by Parker [1972]. This result was combined with a published regional field for the attraction of both topography and root beyond 166.7 km [Kärki *et al.*, 1961] to a distance of 180° on a spherical earth. Although a mismatch exists between the model parameters for the published result of Kärki (sea level compensation depth, 30 km; density contrast, 0.6 g/cm³) and those used for calculation of the root attraction inside 166.7 km (30 km and 0.35 g/cm³), simple calculations suggest that this mismatch causes long-wavelength errors of no more than 5 mGal for most of the onshore conterminous United States. A mismatch of as much as 9 mGal may occur in western Colorado, where a broad area has an average elevation of almost 3 km. Offshore, the maximum mismatch for the very deepest parts of the map area may reach 10 mGal for our

choice of parameters. The obvious future solution to these problems is to calculate the far isostatic field from digital worldwide terrane data.

For land areas, isostatic residual gravity values are subject to errors caused by uncertainty in station elevation, terrain correction, and gravity measurement that probably combine to an uncertainty of less than 2 mGal for most observations. Errors introduced in the calculation of the isostatic regional field are generally less than 5 mGal but locally as much as 10 mGal [Simpson *et al.*, 1986]. We expect that most (probably 95%) of the isostatic residual gravity values calculated on land are accurate to better than 5 mGal, or one half of a color interval in Plate 1. Areas of extreme topographic relief are most likely to contain the larger errors.

Offshore, the grid of Godson and Schiebe [1982] contains free air gravity values. We attempted to continue the Airy-Heiskanen model offshore, and a Bouguer correction was applied to the offshore data by using the 5- by 5-min bathymetric data set to determine water depths. Because of the averaging inherent in this bathymetric data set and because of the 40-km search radius used in preparation of the Godson and Scheibe grid, the mismatch between free air value and Bouguer correction is potentially quite large. We estimate that in areas of extreme sea bottom relief, this mismatch could result in short-wavelength errors as large as 40 mGal, although for most oceanic areas the error is probably less than 10 mGal, or one color interval. We believe that the patterns in the offshore data are sufficiently interesting to warrant keeping these data on the residual map; however, the user should be aware of this problem for areas where bottom depth changes rapidly.

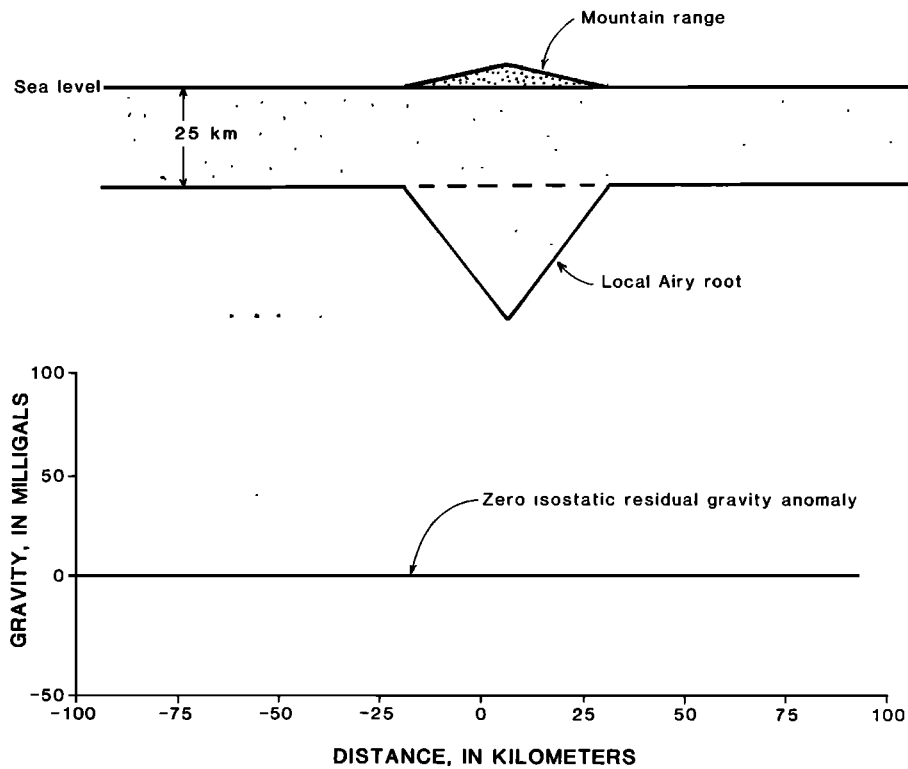


Fig. 7. A 0-mGal isostatic residual anomaly occurs over a mountain that is completely compensated in the local Airy-Heiskanen model. Bouguer correction removes attraction of the mountain range above sea level, and isostatic correction removes attraction of the root, the existence of which is inferred from the topography.

CAUTION ON THE SIGNIFICANCE OF ISOSTATIC RESIDUAL ANOMALIES

There is a common tendency to attribute anomalies on an isostatic residual gravity map to "isostatic imbalances," that is to loads that are either undercompensated or overcompensated. Two sorts of local "imbalance" need to be distinguished. The first kind results from the lateral distribution of compensation that is permitted by elastic strength in the crust and upper mantle. Loads can be supported at a distance so that a regional form of isostatic equilibrium may still obtain, although the compensating masses no longer need to be directly under the loads. Alternatively, areas may be truly out of isostatic balance, even in a regional sense. Such areas, in the absence of elastic support or dynamic processes maintaining the imbalance, ought to be rising or sinking. The present rebound of regions once covered by Pleistocene ice sheets is an example of overcompensation being adjusted by vertical movement. Other correlations of recent vertical tectonic movements with isostatic residual gravity anomalies have been documented [e.g., Kahle *et al.*, 1980].

However, for most individual isostatic residual anomalies less than several hundred kilometers in width, it is not possible, practically, to distinguish these possibilities from gravity data alone or to rule out the third possibility that the particular anomaly is caused by density inhomogeneities in the crust that are completely compensated locally. This point is best made by reference to a simple example. In Figure 7 a mountain resting on a uniform crust is supported by a local Airy-Heiskanen root. On an isostatic residual gravity map, no anomaly would appear because the attraction of the mountain is removed by the Bouguer correction and that of its root by the isostatic correction. In Figure 8 a dense mass in the upper

crust is also supported by a local root. Because there is no topography in this case, the effect of neither the mass nor its compensation has been removed. The compensating mass distribution, because it lies deeper than the mass that it supports, produces a gravity anomaly that is broader and of lower amplitude than that produced by the mass. For the example in Figure 8 the net result is a substantial anomaly, even though the mass is "perfectly" compensated. In principle, the presence of compensating masses could be inferred from the characteristics of the total anomaly: a central anomaly of one sign flanked by broader anomalies of the opposite sign and a total anomaly that integrates to zero. In practice, however, the flanking anomalies commonly are masked by neighboring anomalies and cannot be clearly distinguished.

Longer-wavelength anomalies do not provide much information about isostatic equilibrium either. Many long-wavelength anomalies are caused by sources in the mantle below the depth of compensation and below the classical isostatic system [Dziewonski, 1984; Richards and Hager, 1984]. Intermediate-wavelength anomalies can be modeled by geologically reasonable density contrasts confined to the crust and upper mantle and assumed to be in complete local isostatic equilibrium, as discussed in a later section.

Using Gauss's theorem, it is possible in principle to test for the existence of regional isostatic equilibrium by integrating free air or isostatic anomalies over some appropriate area to obtain a measure of the total anomalous mass in the subsurface. Such an integral ought to approach zero, even in the case of distributed support, if topographic and subsurface loads are compensated by the isostatic mechanism. Our point here is that an individual isostatic residual anomaly does not by itself reveal much about the local existence of undercompensation or overcompensation for its particular source body; it is usu-

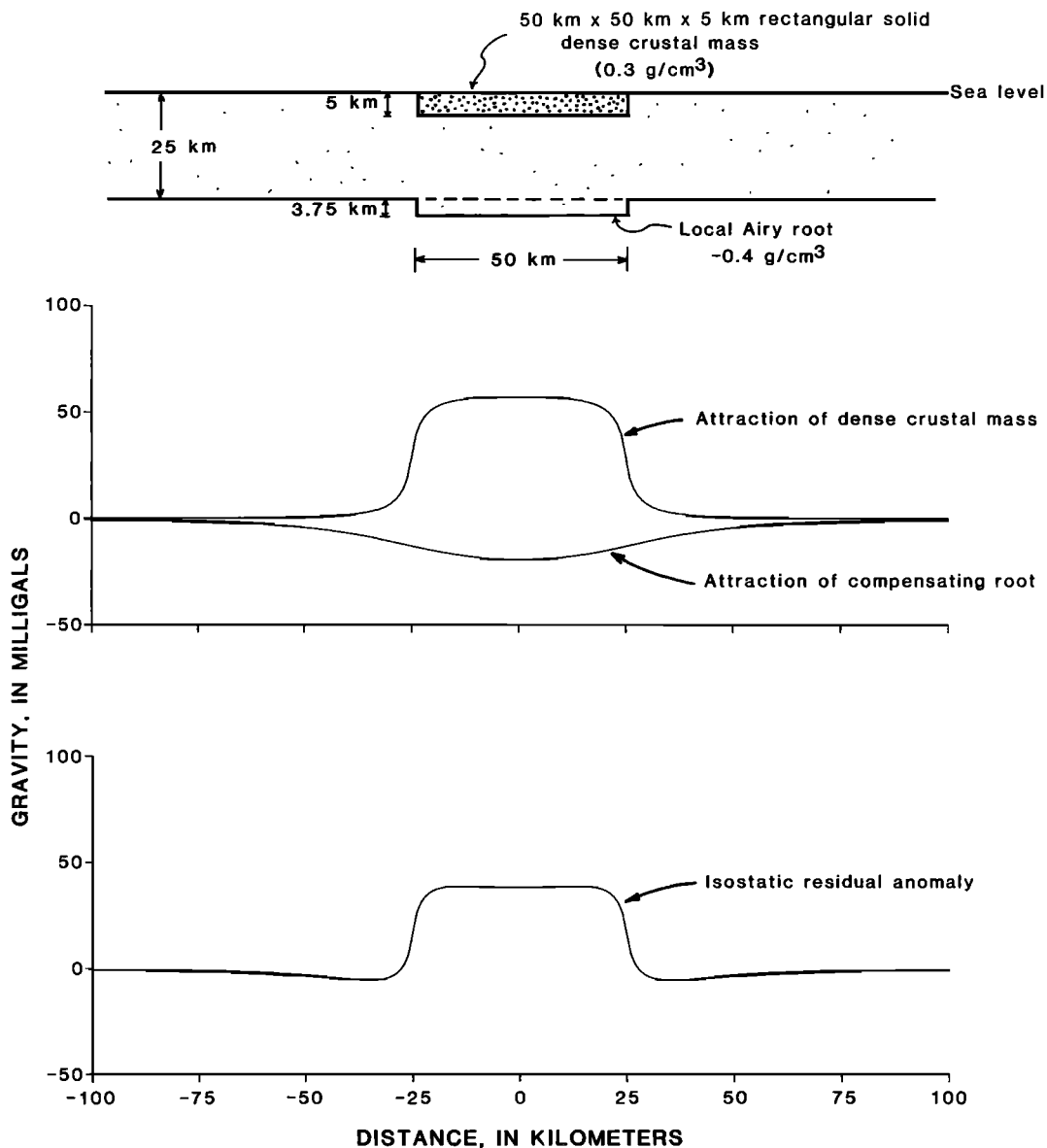


Fig. 8. A large, nonzero isostatic residual anomaly occurs over the center of a dense shallow rectangular mass in the crust, even though it is completely compensated by a local Airy-Heiskanen root. In this case, there is no Bouguer correction because there is no topography above sea level, and there is no isostatic correction for a root, even though one may exist, because the usual isostatic correction only considers the compensating masses under topographic loads. The amount of excess mass in the dense, shallow body is compensated by an equal deficiency of mass in the root; however, the greater depth of the root greatly smooths the gravity low that accompanies the mass deficiency. Thus, when the gravity low is subtracted from the high produced by the dense body, the high remains quite evident in the residual, even though by Gauss's theorem both the low and the high must have equal but opposite volumes under their mathematical surfaces.

ally necessary to appeal to other kinds of geophysical or geological information to decide that question. Isostatic anomalies do, however, tell quite a lot about the lateral distribution of geologically interesting masses in the crust and mantle.

SHORT-WAVELENGTH ISOSTATIC RESIDUAL ANOMALIES

In this section we consider isostatic residual gravity anomalies less than several hundred kilometers wide. Broader anomalies are discussed in the next section. There are both practical and theoretical reasons for making this dichotomy on the basis of anomaly dimension, although the critical width cannot be specified precisely. One practical reason is that many of the prominent gravity anomalies which can be clearly related to geologic or tectonic features are narrower than sev-

eral hundred kilometers; broader anomalies begin to encompass entire geologic provinces. One theoretical reason is that isostatic residual anomalies less than several hundred kilometers wide are quite consistent with a crust in complete local isostatic equilibrium (see previous section), whereas broader anomalies begin to require some special explanation for their existence. In this section and the next, anomalies with one dimension narrower than several hundred kilometers are called short-wavelength (SWL) anomalies.

Many of the SWL anomalies shown on the isostatic residual gravity map can be directly related to known geologic bodies [Woollard, 1966]. We do not attempt to discuss here all the SWL anomalies that appear on Plate 1. Instead, we present a classification scheme that attempts to place most of

TABLE 2a. Sources of Gravity Highs Less Than Several Hundred Kilometers Wide

Geologic-Tectonic Setting	Selected Examples	References
<i>1, Mafic Igneous Bodies: Mostly Autochthonous</i>		
a, Rift setting	a1, midcontinent gravity high	<i>Gabbro, Basalt, and Diorite</i> <i>Craddock et al. [1963], King and Zeitz [1971], Ocola and Meyer [1973], Chase and Gilmer [1973], and Green [1983]</i>
	a2, Wichita Mountains	<i>Mitchell and Landisman [1970], Pruatt [1976], Powell and Phelps [1977], and Brewer et al. [1981]; see also f3</i>
	a3, Michigan high	<i>Hinze et al. [1975] and Brown et al. [1982]</i>
	a4, east continent gravity high	<i>Keller et al. [1982a] and Lidiak et al. [1985]</i>
	a5, East Coast gravity high (partly edge effect also)	<i>Rabinowitz [1974], Rabinowitz and LeBrecque [1977], and Karner and Watts [1982]</i>
	a6, Snake River Plain	<i>Mabey [1976] and Sparlin et al. [1982]</i>
	a7, Appalachian high (? in part)	<i>Cook and Oliver [1981]</i>
b, Magmatic arc	b1, parts of Sierra Nevada	<i>Oliver and Mabey [1963], Oliver [1977], and Griscom and Oliver [1980]</i>
	b2, Peninsular Ranges	<i>Kovach et al. [1962] and Griscom and Oliver [1980]</i>
c, Isolated intrusions: locations probably controlled by structure	c1, south Georgia triplet	<i>Hildenbrand et al. [1982]</i>
	c2, plutons flanking Mississippi embayment graben	
<i>2, Mafic Crust: Mostly Allochthonous Accreted Oceanic or Island Arc Basement or Transitional Basement Formed During Rifting</i>		
d, Large pieces	d1, Oregon and Washington Coast Ranges	<i>Snively et al. [1980]</i>
	d2, parts of the Appalachians	<i>Hutchinson et al. [1983] and Thomas [1983]</i>
e, Small pieces and tectonic slivers	e1, mafic and ultramafic thrust slices in Klamath Mountains and Sierra Nevada	<i>LaFehr [1966] and Jachens et al. [1986a]</i>
	e2, Great Valley high	<i>Cady [1975]</i>
<i>3, Uplifted Crystalline Basement (Dense by Virtue of Original Depth?)</i>		
f, Uplifted by collision or compression on well-defined structures	f1, Laramide Ranges (in part)	<i>Smithson et al. [1979], Hamilton [1981], and Hurich and Smithson [1982]</i>
	f2, parts of Appalachians	<i>Griscom [1963] and Thomas [1983]</i>
	f3, Wichita and, Arbuckle mountains uplift (?)	<i>see references for a2</i>
g, Cause of uplift uncertain (arching or doming?)	g1, Adirondack Mountains	<i>Simmons [1964] and King [1977]</i>
	g2, Llano uplift	<i>Barnes et al. [1954] and King [1977]</i>

the important kinds of isostatic residual anomalies into categories based on the geologic and tectonic settings of their source bodies. Our scheme is presented in Table 2, and the anomalies that serve as examples of the various classes are outlined on Figure 9. This classification presently encompasses only those kinds of gravity anomalies and geologic-tectonic settings that occur within the conterminous United States, although additional classes have been suggested to us by colleagues familiar with the geology of other countries. The list of examples chosen to illustrate the individual categories consists of studies familiar to us and is not intended to be comprehensive or exhaustive. Also, because the classification scheme developed a certain symmetry as it grew, it includes some categories exemplified by rather small anomalies, whereas some of the more conspicuous anomalies about which we know less were not used.

Our classification effort was motivated by the observation of some rather obvious regularities in the causes of certain kinds of anomalies. For example, many of the gravity highs that can be associated with known geologic features seem to be caused by mafic igneous rocks or uplifted crustal sections, and many of the deeper gravity lows seem to coincide with sedimentary basins formed in convergent tectonic environments. As the classification effort progressed, certain irregularities and difficulties in our scheme also became apparent, and some of the categories in Table 2 still do not seem quite appropriate. In the rest of this section we comment on some of the problems that arose in the construction of Table 2 and on some of the anomalies that seemed to offer insights that were new to us. A more comprehensive, area-by-area discussion of SWL gravity anomalies in the conterminous United States has been given by *Kane and Godson [1985]*, although some differ-

TABLE 2b. Sources of Gravity Lows Less Than Several Hundred Kilometers Wide

Geologic-Tectonic Setting	Selected Examples	References
	<i>4, Felsic Igneous Rocks, Including Volcaniclastic Sediment</i>	
h, Batholiths and plutons	h1, Idaho batholith h2, central Wisconsin h3, eastern Sierra Nevada	<i>Hinze [1959], Aiken et al. [1983], and Klasner et al. [1985]</i> <i>Oliver and Mabey [1963], Oliver [1977], and Griscom and Oliver [1980]</i>
i, Volcanic piles: commonly in volcanic depressions	i1, San Juan volcanic field i2, Cascade Range	<i>Plouff and Pakiser [1972]</i> <i>LaFehr [1965] and Blakely et al. [1985]</i>
j, Calderas	j1, Yellowstone j2, Long Valley j3, Timber Mountain	<i>Easton et al. [1975]</i> <i>Kane et al. [1976]</i> <i>Kane et al. [1981b]</i>
	<i>5, Sedimentary Rocks</i>	
k, Extensional settings: Grabens and half grabens	k1, Rio Grande rift (also volcanic rocks) k2, basins in Basin and Range province k3, flanking lows on mid-continent gravity high k4, Triassic basins along East Coast, not shown on Figure 9	<i>Decker and Smithson [1975], Ramberg et al. [1978], and Cordell [1978, 1982]</i> <i>Thompson [1959] and Anderson et al. [1983]</i> see a1 <i>Sumner [1977]</i>
m, Convergent settings: Subduction-related accretionary prisms and basins	m1, offshore Washington and Oregon m2, Great Valley of California m3, Puget Sound	<i>Dehlinger et al. [1968] and Snively et al. [1980]</i> <i>Byerly [1966] and Suppe [1979]</i> <i>Stuart [1961]</i>
n, Convergent settings: Collision and compression-related basins	n1, Laramide basins n2, Ouachita low n3, Appalachian basin n4, Martinsburg Basin, Sevier Basin	<i>Strange and Woollard [1964], Case and Keefer [1966], and Hurich and Smithson [1982]</i> <i>Lyons [1961], Nicholas and Rozendal [1975], Nelson et al. [1982], and Lillie et al. [1983]</i> <i>King [1977] and Karner and Watts [1983]</i> <i>Shanmugam and Lash [1982]</i>
o, Transform-related basins	o1, local basins along San Andreas fault o2, California offshore basins	<i>Chapman and Griscom [1980]</i> <i>Harrison et al. [1966], Blake et al. [1978], and Beyer [1980]</i>
	<i>6, Depressed Crystalline Basement (Less Dense Than Adjacent Basement by Virtue of Crustal Layering?)</i>	
p, Basement downdropped in extensional settings	p1, basement under sedimentary basins of type k	
q, Basement depressed by subduction	q1, basement under sedimentary basins of type m q2, downgoing Gorda plate	<i>Jachens and Griscom [1983]</i>
r, Basement depressed by collisions and compression	r1, basement under sedimentary basins of type n	
s1, Basement depressed in transform settings	s1, basement under sedimentary basins of type o	

ences exist because their anomalies are defined by wavelength filtering rather than by extraction of an isostatic regional.

Comments on Anomalies Over Sedimentary Basins

Sedimentary basins proved to be particularly difficult to classify, possibly because there are so many kinds in so many different tectonic environments [e.g., Bally, 1980]. It might seem that low-density sedimentary deposits, together with the crystalline basement depressed beneath many basins, should combine to produce a gravity low. However, thick sedimentary sections do not always produce gravity lows for at

least three reasons: (1) many sedimentary basins contain thick sections of high-density carbonate rocks [e.g., Hinze et al., 1978] and so the total sedimentary column has an average density close to that for crystalline basement, (2) many broader basins are evidently in isostatic equilibrium, and a broad lens-shaped geometry for the sedimentary deposits is most favorable for the local anomaly to be nearly canceled by the broader anomaly from the compensating masses, and (3) the origin of many kinds of sedimentary basins is related to initial inhomogeneities in the basement or is accompanied by changes in the basement that may produce gravity highs

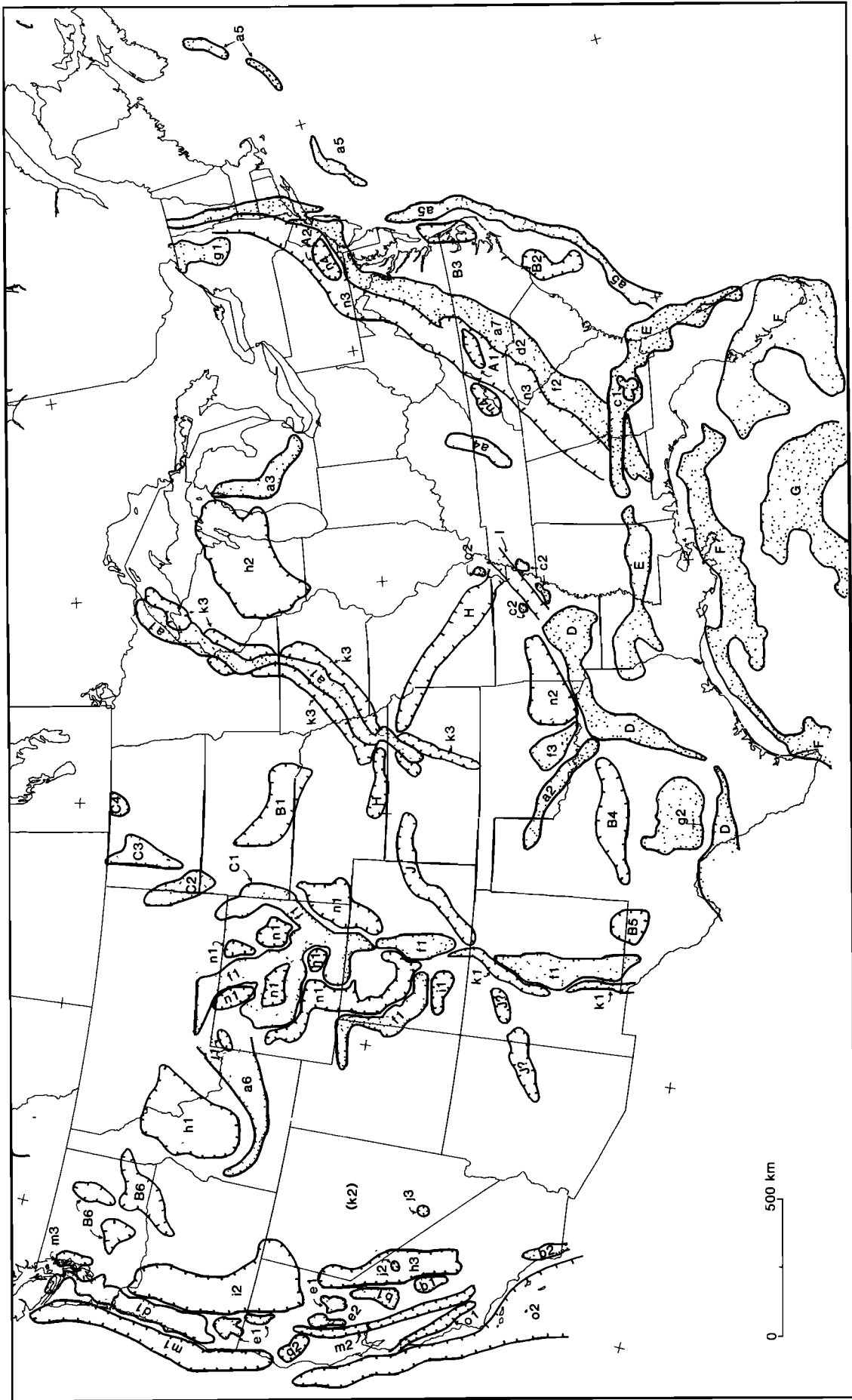


Fig. 9. Index map showing locations of isostatic residual gravity anomalies less than approximately 250 km wide that are discussed in the text. Highs are stippled; lows are hatched. Lowercase letters and numbers refer to categories of anomalies in Table 2; capital letters refer to anomalies discussed in the text.

superposed on lows from the sedimentary section. For example, many basins in the midcontinent area coincide with gravity highs [McGinnis, 1970], probably caused by dense mafic rocks emplaced in the basement during the extensional events that initially triggered the basin formation process [McKenzie, 1978; Sleep and Sloss, 1980]. Because of the number of variables that control the gravity signatures of sedimentary basins, it is difficult to encompass them all in any simple scheme.

Lows Possibly Caused by Sedimentary Rocks Under Allochthonous Sheets

The most conspicuous low anomaly in the conterminous United States is the 100-km-wide low (n2, Figure 9) that occurs in southeastern Oklahoma and western Arkansas. This anomaly is centered over thrust plates exposed in the Ouachita Mountains but extends well to the north over the Arkoma Basin [King and Beikman, 1974; King, 1977]. The boundary of this anomaly on its south-southeast side is a steep, straight gravity gradient that trends obliquely across surface traces of the south dipping thrust plates. The northward extent of the gravity low, the poor correlation between the anomaly and the mapped geology, and the crosscutting relation between its south boundary and structural trends in the Ouachita Mountains all suggest that the source of the anomaly is at least partly concealed beneath allochthonous rocks which have been thrust northward. Seismic reflection profiles in this area [Nelson et al., 1982; Lillie et al., 1983] confirm the existence of a thick sedimentary section at depth under this large gravity low.

In North Carolina the low labeled A1 in Figure 9 may outline another sedimentary basin at depth [Rodgers, 1970, p. 173; A. Griscom, oral communication, 1983]. This low occurs in an area where probable allochthonous Precambrian and Paleozoic crystalline rocks are exposed at the surface [Cook et al., 1979, 1981; Harris and Bayer, 1979]. A nearly identical low anomaly A2 occurs along trend in southeastern Pennsylvania over the Martinsburg Basin [Shanmugam and Lash, 1982] where there is a known thickening of sedimentary deposits above Precambrian basement [Bayley and Muehlberger, 1968; Harris and Bayer, 1979], and so the source of anomaly A1 might be a similar sedimentary basin covered by allochthonous sheets. Shanmugam and Lash [1982] noted that the Sevier Basin in northeastern Tennessee (anomaly n4), which lies about 200 km west of anomaly A1, is an analog for the Martinsburg Basin, further suggesting a connection. The partial overlap of anomaly A1 with the Sauratown Mountains anticlinorium [Williams, 1978] does raise the possibility that structural changes could be responsible for this low, but the similarity in the appearance of anomalies A1 and A2 supports the first possibility. Comparison of these two lows is made possible by the isostatic correction, which, by removing the effects of topography to a first approximation, makes the gravity field of the Appalachians comparable from one end of the chain to the other.

Lows Possibly Caused by Felsic Igneous Rocks

A surprising number of the major gravity lows shown on the isostatic residual gravity map appear to be caused by felsic igneous rocks, consistent with the observation of Bott and Smithson [1967]. Examples are the lows over the Idaho batholith (anomaly h1, Figure 9), over the felsic terrane including the Wolf River batholith in central Wisconsin (anomaly h2), and over the eastern, felsic part of the Sierra Nevada batholith (anomaly h3). The isostatic correction aids considerably in the

comparison of these anomalies because many of them occur in mountainous areas.

Some other major lows shown on Plate 1 are likely to be of similar origin. The large low in South Dakota (anomaly B1, Figure 9) may mark a felsic igneous body because there is no evidence for a sedimentary basin in the basement contours [Bayley and Muehlberger, 1968], at least in the Paleozoic section, and this low is similar in appearance to the low in Wisconsin (anomaly h2), which has been interpreted as reflecting a granitic body [Hinze, 1959]. A similar argument applies to the two lows along the coast of North Carolina (anomalies B2 and B3) because no evidence exists at present for sedimentary basins in the subsurface at the locations of these anomalies [Hutchinson et al., 1982]. The low in north central Texas (anomaly B4) has been attributed to density contrasts within the Precambrian basement [Nicholas and Rozendal, 1975], again suggesting the presence of low-density felsic igneous rocks (perhaps a batholith formed by subduction?). The deep, circular low in western Texas (anomaly B5), which seems to lie along trend with anomaly B4, coincides with part of the Delaware Basin [King, 1977]. Keller et al. [1980, 1982b] have pointed out that the gravity relief between the low (B5) and the high just to the east over the Central basin platform cannot be explained by differences in sediment thickness alone. They suggest a mafic intrabasement mass beneath the Central basin platform to explain the difference, or a low-density intrabasement (felsic?) mass under the basin. The isostatic anomaly values suggest that both kinds of anomalous bodies may be present here.

The gravity lows over the Columbia Plateau (anomalies B6, Figure 9) are likely to be caused at least in part by granite bodies covered by the Columbia River Basalt Group because several of the lows that extend into areas not covered by basalt overlie exposures of granite [King and Beikman, 1974]. However, some of these lows could also be caused by sedimentary deposits under the Columbia River Basalt Group [Stanley, 1984].

Highs Caused by Uplift?

Some of the largest amplitude highs on Plate 1 closely correspond to structural uplifts. The Wichita and Arbuckle Mountains (anomalies a2 and f3, Figure 9) and the Laramide ranges in Wyoming (anomaly f1) provide examples of such structurally elevated blocks that also have present-day topographic expression. We can think of two possible end-member explanations for these gravity highs. The first explanation involves uplift of an anomalously dense body on reactivated structures that may be genetically related to the presence of the dense body; in this case, a gravity high probably existed over the body before uplift occurred. The second explanation relies on an assumed normal increase of density with depth in the crust, related to increasingly higher metamorphic grades and increasingly mafic rock types with depth. In this case, uplift of the crustal section juxtaposes high-density, formerly deep rocks with low-density, upper level crust. No gravity anomaly needs to have existed before uplift. Both explanations may apply to many cases, but it may be difficult to tell which is the more important, as shown below.

The Wichita and Arbuckle Mountains have been described as the site of an aulacogen [Hoffman et al., 1974; Burke, 1980]. One explanation for the gravity highs is that uplift of these mountains, occurring on old lines of weakness associated with the failed rift, elevated dense mafic rocks emplaced along the rift during the early stages of rifting. If so, this anomaly would

seem to be an example of the first type: uplift of a dense body. However, the mafic rocks that are responsible for the gravity highs [Pruatt, 1976] are apparently older than previously thought and are probably unrelated to the Cambrian igneous rocks that floor the thick Paleozoic sedimentary section in the aulacogen. These mafic igneous rocks are part of an eroded stratiform gabbro complex of probable Precambrian age [Powell and Fischer, 1976; Powell and Phelps, 1977; Powell et al., 1980]. Although an older age for these rocks may simply indicate an earlier origin for the aulacogen than was previously thought [Gilbert, 1983], we speculate that the stratiform mafic rocks may predate formation of the aulacogen. If so, their original geometry was probably not elongate and linear, and other parts of this complex may still be present at depth to either side of the present surface exposures. This speculation is consistent with the following observations: (1) The Wichita and Arbuckle mountains lie at the southwest margin of a broad regional area of high gravity values, centered over the Mississippi embayment (Plate 1). In the next section we interpret this broad area to indicate a region of higher than average crustal density. (2) The gravity highs over the Arbuckle Mountains, which are similar in shape and size to those in the Wichitas where the stratiform complex is exposed, seem to ramp down on a gentle gradient to the north, where they merge with the regional high. (3) Seismic reflection data establish the presence of conspicuous subhorizontal reflectors in the Precambrian basement to the south of the Wichita Mountains [Brewer et al., 1981]; one study has attributed these reflectors to igneous bodies [Lynn et al., 1981]. Therefore we suggest that in this case the highs may be caused by uplift on major structures of dense stratiform mafic rocks that occur over a broad area in the subsurface. Clearly, many important details still remain to be established.

Highs Predating Uplift?

The gravity highs over the Laramide ranges in Wyoming and the lows over the intervening basins form one of the most distinctive patterns of anomalies shown on Plate 1. It seems logical to ascribe the highs to uplift of dense lower crustal rocks. In fact, the amplitudes of the highs over Laramide uplifts in New Mexico, Colorado, Utah, and Wyoming correspond well to the amount of Laramide crustal shortening proposed by Hamilton [1981] for these areas. However, an interesting (though speculative) chain of argument suggests that the gravity highs over the ranges in Wyoming may in part predate formation of the topographic ranges during the Laramide orogeny. In other words, if a paleogravity map could be constructed for Wyoming by restoring the crust to its state before the Laramide orogeny, then gravity highs might be found that would, at least in part, coincide with the present highs. A similar conclusion was reached by Case and Joesting [1972, p. 28] for gravity anomalies associated with Laramide structures on the Colorado Plateau.

The argument goes as follows: the high anomalies in the Dakotas (C1-C4, Figure 9) seem to be natural echelon extensions of the highs associated with the Laramide ranges (f1). Although it is tempting also to ascribe these anomalies to Laramide uplift, basement contour maps [Bayley and Muehlberger, 1968] do not support this interpretation. The gravity high over the Black Hills uplift of Laramide age (anomaly C1) extends northwestward with an amplitude that seems too large to be explained by structural upwarp of the basement; this high appears to reflect, at least partly, an intrabasement

source, though one that is closely associated with the uplift. The high over the Williston Basin (anomaly C2) appears to lie over an anticline in the subsurface that was formed during the Precambrian and subsequently reactivated during the Paleozoic and again in the Mesozoic during the Laramide orogeny [Gerhard et al., 1982]. Existing relief on the basement surface does not seem adequate to explain the amplitude of the observed gravity high. Anomaly C2 lies on an electrical conductivity anomaly that wraps around the Black Hills and extends northward into Canada, where it extrapolates into an exposed shear zone that may follow a Proterozoic plate boundary [Camfield and Gough, 1977]. Because many Precambrian plate boundaries have linear gravity anomalies associated with them [Gibb et al., 1983], the source of anomaly C3 could well lie in the basement and reflect a Precambrian suturing event. Similarly, highs C3 and C4 lie close to the extrapolation of the Nelson River high in Manitoba which parallels the boundary between the Superior and Churchill Precambrian provinces for at least 900 km in Canada [Gibb, 1968; Green et al., 1979, 1985].

Thus one explanation for the similarity between anomalies C1-C4 and the highs over the Laramide uplifts in Wyoming is that they all partly reflect basement inhomogeneities or structures that predate the Laramide orogeny: structures that were reactivated by compression to create the present ranges, thereby enhancing preexisting gravity highs. This view is supported by the presence in southeastern Wyoming of a northeast trending Proterozoic suture [Johnson et al., 1984; Karlstrom and Houston, 1984], reactivated during the Laramide, that seems to control the location of conspicuous gravity highs in this part of the state and that merges into the electrical conductivity high which wraps around the Black Hills. Locally along this suture, major highs occur over exposed mafic intrusions and anorthosites that probably owe their origin to the suturing process.

High-Low Anomaly Pairs Marking Possible Collisional and Accretionary Events

Paired linear high-low anomalies commonly form the gravity signature of plate tectonic sutures [Gibb and Walcott, 1971; Gibb and Thomas, 1976; Gibb et al., 1983]. Finding the cause of these paired highs and lows is not always simple, although the following factors are frequently mentioned. Lows marking sutures may be caused by (1) sialic crust downwarped by the weight of thrust plates [Karner and Watts, 1983], (2) accumulations of sedimentary deposits in the downwarped areas, and (3) belts of granitic intrusions [Gibb, 1968]. Highs can be formed by (1) dense accreted terranes (e.g., island arcs, oceanic basement), (2) mafic rocks emplaced during the early rifting event that formed a continental margin now altered by collision [Cook and Oliver, 1981; Lillie, 1985], and (3) dense rocks upthrust by the collision (potentially either dense lower crustal rocks, dense mafic rocks formed during an earlier rifting event, or dense accreted rocks).

In the Appalachian orogen the 3000-km-long high-low pair (anomalies labeled a7, d2, f2, and n3, Figure 9) has been studied by many workers, but its source and tectonic significance remain unclear. We suggest the following points to be of central importance in any attempt to understand this anomaly:

1. The high-low pair and the gravity gradient between them parallel a fundamental plate tectonic boundary. A good case can be made that this boundary is the eastern edge of the

late Precambrian–early Paleozoic North American continent [Rodgers, 1970; Cook and Oliver, 1981].

2. Major differences in crustal thickness and density exist on either side of the gradient [Hutchinson et al., 1983; Thomas, 1983].

3. In several places, local highs within the area of the major high anomaly coincide with exposed dense, often mafic, rocks [Best et al., 1973; Dainty and Frazier, 1984]. The occurrence of far fewer local highs within the area of the major low suggests that the sources of the high anomaly are partly shallow. If the fundamental source of the anomaly is to be placed at depth, especially below a décollement surface, then the coincidence of local highs at the surface with the area of the main high demands explanation.

4. In places, local highs can be identified with mafic igneous rocks of Ordovician age, a relation suggesting that the high-low pair is related to an Ordovician (Taconic) collision of an island arc with the North American continent [Griscom, 1963]. Subsequent collisions may have altered these anomalies to some degree.

5. In several places the gravity gradient locally follows mapped structures and exposed boundaries between terranes [cf., Williams, 1978; Haworth et al., 1980], and structures to the west of the gradient generally are subhorizontal, whereas those to the east are steeper [Griscom, 1963]: again, a relation suggesting that the sources are in part shallow.

Many early discussions of the Appalachian paired high-low did not take adequate account of its complexity along strike, mostly because these studies were based on older regional gravity maps that failed to resolve much important detail. In several places, two or more gradients are encountered as one traverses the high-low pair. A good example of this occurs in Virginia, where the westernmost gradient closely parallels the hingeline of the early Paleozoic continental margin [Wehr and Glover, 1985]. (A gradient analysis [Blakely and Simpson, 1986] suggests a continuation to the southwest, with a change in polarity, toward the gravity high in the southwest corner of North Carolina.) A second gradient to the east of the first can be followed through central North Carolina into southern Virginia. Using earlier, less detailed gravity maps, various workers have drawn a connection across southern Virginia between these two gradients. The resulting connection is somewhat haphazardly related to surface geology. We think that these two gradients are presently quite distinct, although the westernmost gradient in Virginia and the gravity high in southwestern North Carolina may be caused by rocks transported to the west during Alleghenian thrusting, so that these rocks may have at one time contributed to a more continuous, less dismembered post-Ordovician gravity high-low pair.

The source of the gravity high in the Appalachians seems to us central to the problem of discovering the tectonic significance of the Appalachian high-low pair, and this source has not, to our minds, been entirely sorted out yet. The three possible explanations given above for the highs in paired anomalies (a dense terrane juxtaposed by accretion, mafic rocks emplaced during an early rifting episode, or dense rocks uplifted by thrusting during collision) all probably play a role in the creation of the high, and the relative contributions may change along strike, depending on the irregularities in the colliding margins, or other factors. Much progress could be made in evaluating these causes if more models were constrained by density measurements of rocks exposed at the surface.

Other paired anomalies shown on Plate 1 may indicate sites of former collisions. The gravity highs and flanking lows (immediately adjacent to the west and north) that extend across Texas, Oklahoma, and Arkansas (anomaly D, Figure 9) probably record the collisional event that formed the Ouachita System [Nicholas and Rozendal, 1975; Lillie et al., 1983]. Another anomaly pair, consisting of an irregular high (anomaly E) and somewhat scattered lows on the north side, that extends from southern Georgia to Louisiana could also mark a collision-accretion event. Aeromagnetic data for this area have been interpreted in terms of an Alleghenian suture [Horton et al., 1984] along this trend. The apparent continuation of the northeast trending Appalachian high across this east-west high may simply indicate that the east-west suture is a low-angle fault which has carried the accreted terrane labeled E over the south end of the Appalachian orogen, and the Appalachian feature may extend in the subsurface several hundred kilometers to the south of the northern margin of the accreted terrane.

The paired anomalies consisting of the high just offshore along the Gulf Coast and the parallel low to the north along the south margins of the Gulf States (anomaly F, Figure 9) could indicate another suture. However, the interpretations of tectonic events in the Florida area presented by Klitgord and Popenoe [1984] and Pindell [1985] suggest that anomaly F and the large anomaly G to its south may be related to rifting, extension and attenuation of continental crust, and formation of oceanic crust during Jurassic time.

Two Linear Lows Probably Related to Structures

The northwest trending linear low extending from Missouri to Nebraska (anomaly H, Figure 9) has been attributed to a Precambrian structure, possibly a failed rift [Guinness et al., 1982]. If this is a rift, it is clearly at a very different stage of development or of a very different sort than several other rifts marked by prominent gravity highs (e.g., the midcontinent rift a1). Although the source of this anomaly (H) is uncertain, it has great potential importance for understanding intraplate earthquakes occurring in the midcontinent because the intersection of this anomaly with the Mississippi embayment graben [Kane et al., 1981a; Hildenbrand, 1985] contains the epicenters of present microseismicity in the New Madrid, Missouri, area [Arvidson et al., 1982].

A second linear low (anomaly J, Figure 9) extends northeastward from northern New Mexico, across the southeastern corner of Colorado, into Nebraska, where it almost joins with the Missouri-Nebraska low. (Anomalies J? are possible extensions to the southwest into Arizona.) This second low is similar in appearance to the first (anomaly H), though not quite so straight, and it may also indicate a Precambrian structure. It could be part of a high-low pair (with the somewhat ragged high on the southeast side) over a Precambrian suture zone, although the nearest Precambrian province boundary, as presently known, lies parallel to the low but about 100 km to the southeast [Van Schmus and Bickford, 1981; Karlstrom and Houston, 1984]. The manner in which this low seems to merge with some of the lows along the Rio Grande rift valley suggests that the position of the Rio Grande rift in part of northern New Mexico may have been controlled by this ancient structural trend. The northeast trending Jemez lineament in northern New Mexico [Aldrich et al., 1984] could be a southwestward continuation of the trend. This lineament, which controlled the locus of much of the volcanic activity in north-

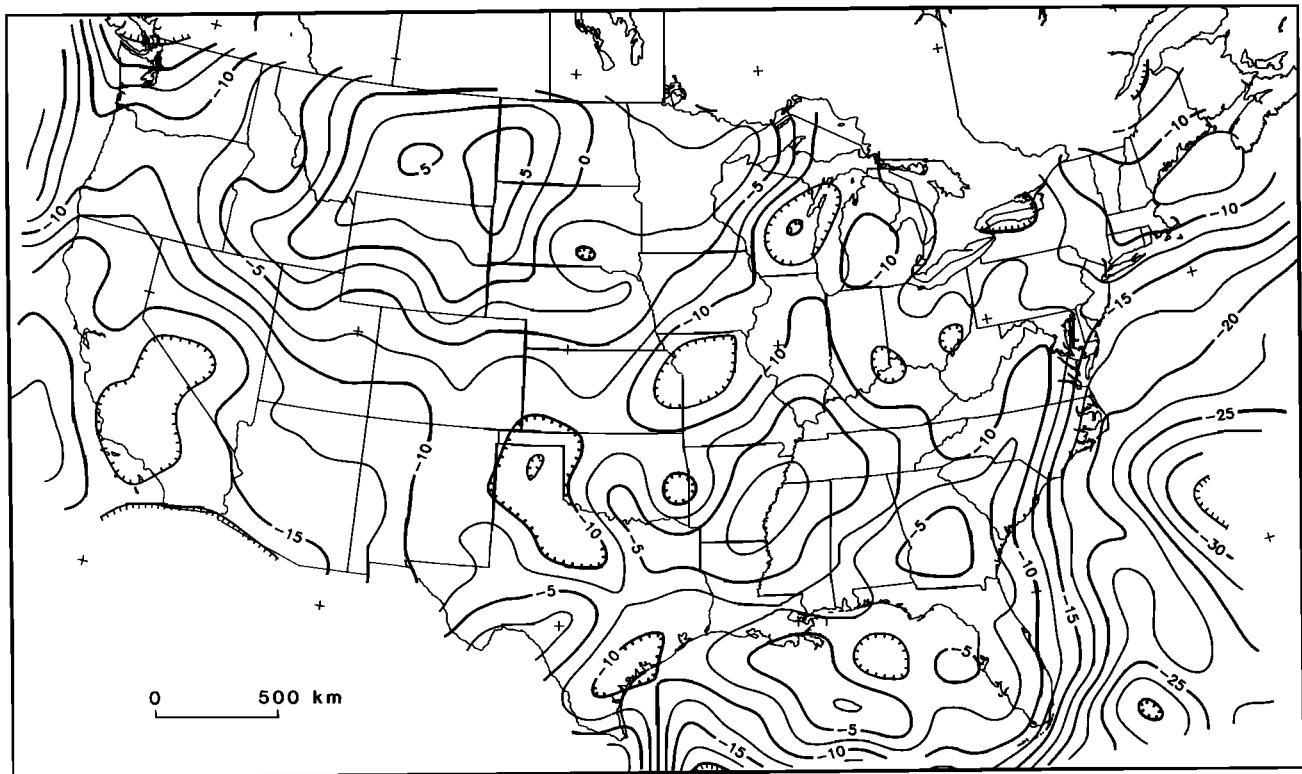


Fig. 10. Isostatic residual gravity field, upward continued to 150 km. Smoothing of shorter wavelength anomalies aids in the identification of longer-wavelength features. Contour interval, 2.5 mGal. Hachures on inside of closed contours enclosing gravity minima.

ern New Mexico during the Tertiary, appears to be a reactivated Precambrian structure and, possibly, a boundary between Precambrian provinces of different age [Aldrich *et al.*, 1984].

SOURCES OF BROADER ISOSTATIC RESIDUAL ANOMALIES

Many of the broader anomalies in the earth's gravity field are undoubtedly caused by density contrasts deep in the mantle or core [Bowin, 1983] below the classical levels of isostatic compensation, and new seismic techniques are beginning to resolve velocity contrasts that probably define these deep source bodies [Clayton and Comer, 1983; Dziewonski, 1984; Richards and Hager, 1984; Woodhouse and Dziewonski, 1984]. Anomalies of intermediate wavelength (IWL), ranging from several hundred to several thousand kilometers in width, can be caused either by sources below the lithospheric plates or by sources within the plates, although this second possibility requires, because of the widths involved, that special attention be given to the question of isostatic equilibrium.

In this section we explore the possibility that all of the IWL anomalies shown on Plate 1 might be caused by lithospheric sources which are in isostatic equilibrium. Two lines of argument can be used to support this contention: (1) geologic evidence suggests that many of the broader anomalies shown on Plate 1 correlate with Precambrian provinces or tectonic terranes, and (2) simple models demonstrate that such anomalies can be produced by geologically reasonable density contrasts which are in local isostatic equilibrium and confined to depths of less than 100–200 km.

Several IWL anomalies, ranging from several hundred to several thousand kilometers in width, are apparent on Plate 1 and in Figure 10. For example, Montana, Wyoming, and the

Great Plains region to the west of the midcontinent gravity high (MGH) are more positive (redder) than average (Figure 11), as is an area centered around the Mississippi embayment. On the other hand, the intervening region extending from northern Texas to Wisconsin is mostly lower (greener) than average. Oceanic crust of Mesozoic age in the western Atlantic Ocean coincides with generally low isostatic residual gravity values, whereas crust of Cenozoic age belonging to the Juan de Fuca plate and other small oceanic plates offshore from Oregon and Washington has higher residual gravity values.

These broad anomalies are not likely to be artifacts of the isostatic correction process or of the particular parameters used to generate the isostatic residual maps shown here because the same broad anomalies are apparent on colored versions of the free air gravity data [McGinnis, 1979; Bowin *et al.*, 1982; Simpson *et al.*, 1983b], and some of the larger ones are apparent on free air gravity maps inferred from satellite-derived geoids [Lerch *et al.*, 1979]. Long-wavelength (LWL) biases can be introduced into gravity data by reducing the data to the geoid (sea level) rather than to the reference ellipsoid [Chapman and Bodine, 1979]. A correction can be applied to remove this so-called indirect effect and the attraction of the slab of material between the geoid and the ellipsoid. This correction equals approximately 0.2 mGal/m on land for a reduction density of 2.67 g/cm³. For the conterminous United States the geoid relief is approximately 30–40 m [Lerch *et al.*, 1979; Chapman and Talwani, 1979], and so the maximum relative correction is about 8 mGal. The sign of this correction is such that it increases the amplitude of LWL anomalies: in the northern Rocky Mountains area, where the geoid is 10–20 m higher than it is over most of the eastern United States, the corrected amplitudes have 2–4 mGals of additional relief.

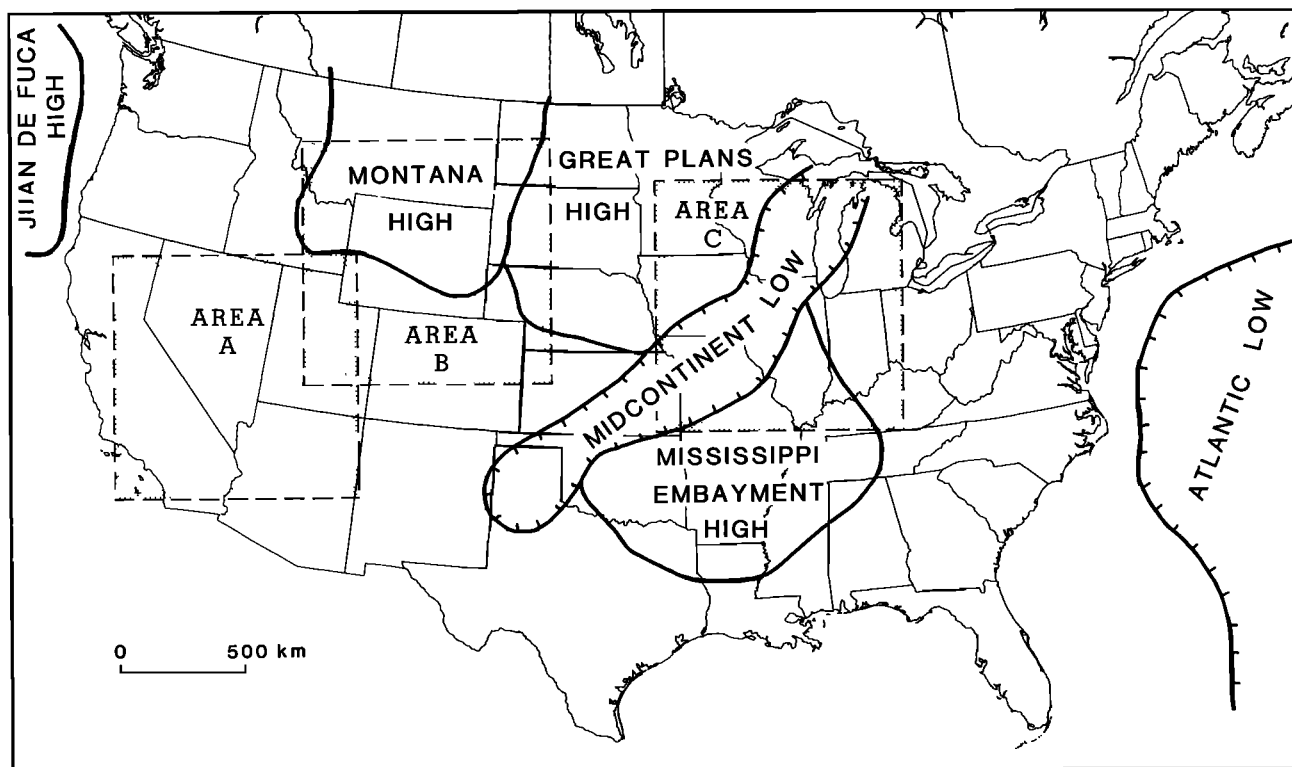


Fig. 11. Index map identifying certain longer-wavelength isostatic residual gravity anomalies discussed in the text. Boundaries are approximate. Hachures appear on inside of boundaries enclosing areas of low gravity values. Dashed squares show locations of the three areas (A-C) of the isostatic residual gravity map studied by spectral analysis. Each area has dimensions of 1000 by 1000 km.

Thus the indirect effect is too small to change in any important way the positions or amplitudes of the broad anomalies shown on the isostatic residual map.

Correlations of Some Broad Anomalies With Crustal Geologic Features

Several lines of geologic and geophysical evidence suggest that at least some IWL isostatic residual gravity anomalies are caused by shallow density contrasts, as first emphasized by Woollard [1972, 1976]. For example, the large high over Montana and adjacent states is part of a broad anomaly extending into Canada that is clearly displayed on satellite free air gravity maps [Kaula, 1972; Lerch *et al.*, 1979]. Although such a broad anomaly, approximately 1000 km wide, could have its source in the mantle, the coincidence of several geologic features with parts of the high suggests that its sources lie at least partly in the crust. An accreted Precambrian terrane containing a large block of crust of Archean age may form the basement for the region of Montana, Wyoming, and Idaho under the high anomaly [Dutch, 1983]. This basement was reactivated by Laramide compressional events [Hamilton, 1981], and uplifted pieces cause the conspicuous linear gravity highs in Wyoming. Seismic refraction experiments [Woollard, 1972; Allenby and Schnetzer, 1983] indicate an area of abnormally thick, high-velocity crust and upper mantle in places under the anomaly.

In some tectonic contexts, density contrasts might reasonably be expected to exist both in the mantle and in the overlying crust: a hotspot originating deep in the mantle might bring to the surface mafic igneous materials and produce an upward bulge; a low-angle subducting slab overridden by a continent might extensively modify the continental lithosphere

by compression, underplating, or tectonic erosion over large distances [Bird, 1984]. However, most such paired deep and shallow density contrasts must eventually be separated by the motions of the plates. If some of the sources for the broad gravity high centered over Montana can be convincingly associated with crust of Precambrian age reactivated by later tectonic events, then it becomes likely that the entire anomaly is generated by sources lying in the lithospheric plate. This anomaly may contain interesting information about the origin and composition of the terranes involved, their accretion, and their subsequent reactivation.

Another example of the possible correspondence of IWL anomalies with geologic terranes can be found in the midcontinent region. Except for a few areas of exposed Precambrian rocks, the Precambrian basement in this region is hidden under younger sedimentary strata. The evidence for the extent of different Precambrian provinces in the midcontinent region consists mostly of lithologic, geochemical, and isotopic determinations on core samples obtained from scattered drill holes. The characteristics of the various provinces and the province boundaries are becoming better defined as more data become available [Denison *et al.*, 1984; Karlstrom and Houston, 1984; Dutch, 1983; Van Schmus and Bickford, 1981; Condie, 1982]. A correlation between IWL gravity anomalies and Precambrian provinces is suggested by the facts that (1) the edges of these broad anomalies are sometimes quite abrupt and sharply defined, which requires that the source bodies at least extend up into the crust in places, and (2) the edges of some of these anomalies coincide with known Precambrian tectonic features.

For example, a step in the regional base levels of gravity values occurs across the southern end of the MGH. Gravity values over a broad region to the northwest of the MGH

average 20–30 mGal higher than those over the region to the southeast. It is unlikely that any large part of the midcontinent area is greatly out of isostatic balance given the speed of glacial rebound [Cathles, 1975]. The high region to the northwest (Great Plains high, Figure 11) probably has as its basement the extensions of Archean and early Proterozoic Precambrian provinces that are exposed in surrounding areas [Dutch, 1983; Klasner and King, 1986; Green et al., 1985]. The gravity low to the southeast nearly coincides with one or more felsic Precambrian terranes that were probably sutured to the terranes to the northwest sometime after about 1700 Ma [Bickford et al., 1981b; Dutch, 1983; Thomas et al., 1984]. (Anomaly J on Figure 9 may mark one of these suture boundaries.)

The width of the gravity step across the south end of the MGH, though obscured by the presence of the MGH along part of its length, is sufficiently narrow to indicate causative density contrasts no deeper than 50 km. The MGH is traditionally interpreted to overlie a rift of Precambrian age, and the gravity high is probably caused by mafic igneous rocks associated with the rifting [Craddock et al., 1963; King and Zietz, 1971; Chase and Gilmer, 1973; Ocola and Meyer, 1973; Green, 1983]. The coincidence of the change in gravity base level with the south end of this first-order geologic feature must be more than fortuitous. Because rifting commonly occurs along or near the lines of old sutures that continue to be zones of weakness, the southern part of the MGH rift may have begun to open along an old suture between two Precambrian terranes that had been rafted together earlier. In any event, the high gravity base level to the west and the low base level to the east probably indicate crustal sections of more mafic and more felsic composition, respectively. The density contrasts responsible for this change in gravity base level probably do not extend below the bottom of the lithosphere, because the North American plate has moved thousands of kilometers over the asthenosphere since the Precambrian.

The northeast trending gradient between the midcontinent low and the Mississippi embayment high (Figure 11) is a second example of a boundary between IWL anomalies corresponding to a geologic feature. This gradient approximately follows the boundary drawn by Bickford et al. [1981a] between a terrane to the north consisting of abundant granite and metavolcanic and metasedimentary rocks and a terrane to the southeast consisting of rhyolitic flows, ash flow tuff, and epizonal granite plutons. The gravity data suggest that the terrane to the southeast underlies a large part of the Mississippi embayment area and that it must have a denser crustal and upper mantle section, on average, than the terrane to the northwest, even though from subsurface sampling both terranes are characterized as felsic.

Constraints Imposed by Isostatic Equilibrium

We now consider whether or not these IWL anomalies can be caused by density contrasts within the lithosphere that are in isostatic equilibrium. We assume for the moment that all such anomalies have sources in the crust and upper mantle (even though this may not be the case for all such anomalies) and investigate the implications. Although an isostatic correction has been made for topographic loads in the construction of Plate 1, no such correction has been applied for the compensation that exists for loads caused by anomalous densities within the crust or upper mantle. To test the worst case, we ignore the possibility of distributed compensation and assume that local isostatic equilibrium applies, even though the litho-

sphere has in many areas sufficient strength to support sizable loads over distance of hundreds of kilometers for probably billions of years [Lambeck, 1980; McNutt, 1980; DeRito et al., 1983]. Lithospheric strength allows the compensating masses to be distributed more broadly. Local compensation is an extreme case, in the sense that any acceptable local compensation model consistent with the observed gravity field can probably be replaced by a distributed-compensation model that has the compensating masses at shallower depths. Distributed compensating masses will generally produce smoother isostatic regional fields than will local compensating masses at the same depth.

In our very simple compensation model we will assume that IWL anomalies are produced by density contrasts in the crust and upper mantle which are locally compensated by density contrasts of the same geometry but opposite sign at a depth d below the upper contrasts. We can then make a second-order isostatic correction in which we remove not the roots to topographic loads (which were removed by the first-order isostatic correction used in Plate 1) but the roots to massive bodies within the crust. This operation is easily accomplished for our simple compensation model (on a flat earth) in the Fourier transform domain. The Fourier transform of a function $u(\mathbf{s})$ is given by

$$\mathcal{F}[u(\mathbf{s})] = \int_{-\infty}^{\infty} \int_{-\infty}^{\infty} u(\mathbf{s}) e^{-i\mathbf{k}\cdot\mathbf{s}} dx dy \quad (3)$$

In the following analysis, $\mathbf{s} = (x, y)$ and $\mathbf{k} = (k_x, k_y)$ represent horizontal coordinates in the two-dimensional space and Fourier domains, respectively, and $k = |\mathbf{k}|$. We assume that the observed anomaly field $a_{\text{observed}}(\mathbf{s})$ is the sum of the anomaly field produced by loading sources in the crust and upper mantle and by compensating sources at greater depth:

$$a_{\text{observed}}(\mathbf{s}) = a_{\text{loading}}(\mathbf{s}) + a_{\text{compensating}}(\mathbf{s}) \quad (4)$$

(This separation raises some interesting questions about when a mass embedded in the crust can be considered a loading mass or a compensating mass. Such questions become irrelevant in models that integrate the density distributions with the mechanical and rheological properties of the lithosphere and their variations in space and time.) The compensating mass distributions are assumed to have the same geometry as the upper level mass distributions, density contrasts opposite in sign, and depths greater by distance d . Therefore

$$\mathcal{F}[a_{\text{compensating}}(\mathbf{s})] = -e^{-kd} \cdot \mathcal{F}[a_{\text{loading}}(\mathbf{s})] \quad (5)$$

Substituting this expression into the Fourier transform of (4),

$$\mathcal{F}[a_{\text{loading}}(\mathbf{s})] = \frac{\mathcal{F}[a_{\text{observed}}(\mathbf{s})]}{1 - e^{-kd}} \quad (6)$$

Thus, in this simple compensation model the observed anomaly can be separated into the part produced by the loading masses and the part produced by the compensating masses. The postulated compensation geometry is artificial, but because of the smoothing effect of the greater distances to the compensating masses, it provides an acceptable second-order isostatic correction. We ignore for present purposes the possible interactions of the compensating masses from the first- and second-order isostatic corrections and assumed that these corrections can be made independently.

As a final step toward investigating the reasonableness of isostatic balance for IWL anomalies, the gravity anomalies

caused by the loading masses alone (equation (6)) can be converted into equivalent density contrasts $\rho(s)$ varying laterally within a layer of thickness t starting at the earth's surface:

$$\mathcal{F}[\rho(s)] = \frac{k}{2\pi G} \frac{\mathcal{F}[a_{\text{loading}}(s)]}{1 - e^{-kt}} \quad (7)$$

The inverse Fourier transform applied to equation (7) gives a density distribution in a layer of thickness t that produces the observed (first-order) isostatic residual gravity field and is in complete local isostatic equilibrium. The question then becomes whether or not the density distribution so calculated is geologically plausible.

If the loading masses are confined to a thickness of 50 km and the compensating masses are confined to the layer from 50 to 100 km, then the level change in gravity values across the MGH can be explained by density contrasts of 0.10–0.15 g/cm³. Although such contrasts are not unreasonable in comparison with the ranges of typical densities for igneous and metamorphic rock suites [e.g., *Gibb*, 1968], geologically the persistence of such a contrast down to 50 km would require fundamentally different crustal sections for the areas on either side of the step. The true density contrast need not be distributed uniformly throughout the entire 50-km layer, of course; higher density contrasts in only a part of the section could also satisfy the constraints.

If the layer with loading sources is 100 km thick and the compensating layer extends from 100 to 200 km, the step across the MGH can be satisfied by density contrasts of only 0.05–0.10 g/cm³ in the upper 100 km. These density contrasts are even easier to explain geologically, although in this case they would need to extend across fundamental geologic discontinuities such as the M discontinuity. This 100-km model has the further property that all the broad anomalies across the continent, including the great high centered over Montana, can be explained in terms of density contrasts of less than 0.1 g/cm³ in an upper layer 100 km thick. (Features requiring greater or lesser contrasts than this are all narrower than 200 km.) All areas are again in local isostatic equilibrium, with compensating masses extending from 100 to 200 km in depth.

The loading density contrasts can be confined to shallower levels if the compensating masses are permitted to lie deeper. For example, if loading density contrasts are restricted to a 50-km-thick crustal layer and compensating masses are confined between 200 and 250 km, then the range of density contrasts required in the upper 50-km-thick layer is nearly identical to the last model. Doubling the depth of the compensating layer and halving the thickness of the loading layer produce effects that cancel to first order. Compensating masses could conceivably exist at such depths and still be part of the moving tectonic plate; *Jordan* [1978] argued that attached root zones exist to depths of hundreds of kilometers beneath the old continental nuclei in a continental tectosphere. For the Wyoming area, such a deep inherited root would not fit well with the slab geometries postulated by *Bird* [1984] for an episode of Laramide crustal thickening.

One conclusion suggested by these hundred-kilometer depths is that isostatic compensation may occur at several levels or over a broad range of depths in the upper mantle. The mechanical properties of felsic continental crust over mafic mantle material are consistent with the presence of two weak zones at depths determined by the thermal gradient and mechanical properties of quartz and olivine, respectively

[*Brace and Kohlstedt*, 1980]. Gravity studies of the transition from the Basin and Range to the Colorado Plateau [*Zoback and Lachenbruch*, 1984] indicate that compensation may be partly achieved by variations in the lithosphere thickness.

Although our simple models suggest that many of the IWL anomalies shown on Plate 1 could have sources in the lithosphere and still be in isostatic equilibrium, gravity studies alone cannot answer many of the questions raised here about the vertical distributions of density contrasts. Density models consistent with the gravity data must be constrained by other types of information on the strength and movement of the materials that support the density contrasts and by other types of geophysical data more sensitive to vertical variations in the crust and mantle than the gravity data. Recent developments in seismic tomography appear to hold great promise in these areas.

THE FIRST-VERTICAL-DERIVATIVE MAP

Plate 3 shows the first vertical derivative of the isostatic residual gravity field (also upward continued 10 km to suppress some the SWL noise generated by the derivative). The first vertical derivative [*Hildenbrand*, 1983] enhances shorter wavelengths and suppresses longer wavelengths and is accomplished by multiplying the Fourier transform of a potential field map by the wave number k . The effect is to sharpen anomalies caused by abrupt lateral changes in near-surface densities at the expense of broader anomalies caused by deeper or more gradual density changes. For this reason the map is useful for comparison of anomalies with geologic bodies exposed at the surface. Suppression of longer wavelengths also aids in comparing and distinguishing trends and anomaly fabrics in various domains. The work of *Hildenbrand et al.* [1982] in defining the Mississippi embayment graben provides a good example of the enhancements offered by applying vertical derivatives to potential field data.

Applying the first vertical derivative is also equivalent to a pseudomagnetic transform: the first-vertical-derivative value is proportional to the magnetic anomaly that would be observed if dense material were replaced by magnetic material in exact proportion and if the magnetization direction and the local geomagnetic field direction were oriented normal to the earth's surface. Because of this property, the map can be usefully compared with maps of aeromagnetic anomalies (preferably reduced to the pole). Several important rock groups can be distinguished by the coincidence (or noncoincidence) of aeromagnetic and gravity anomalies. For example, many mafic rocks are both dense and magnetic, as can be seen by comparing Plates 1 and 3 with the aeromagnetic map [*Zietz*, 1982] and the geologic map [*King and Beikman*, 1974] of the United States.

DISTINGUISHING DOMAINS BY SPECTRAL ANALYSIS

Various regions of the isostatic residual gravity map of the United States (Plate 1) exhibit characteristic patterns, trends, and fabrics of anomalies. Much of the Basin and Range province, for example, is characterized by a pattern of SWL (10–50 km wide) anomalies reflecting individual basins and ranges, whereas the midcontinent region is composed of longer-wavelength (50–100 km) anomalies often lineated for great distances. It would be useful to quantify the differences between regional anomaly patterns because they may distinguish terranes with specific origins or tectonic histories. Fourier analysis is one quantitative approach: anomalies of various

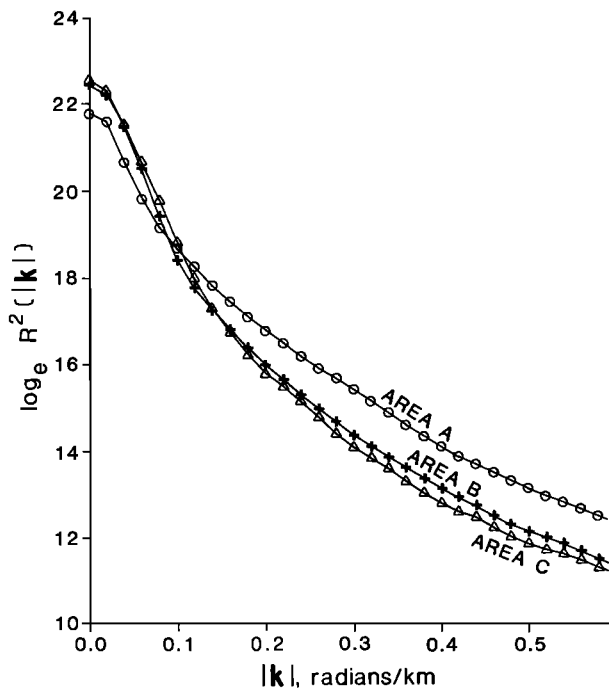


Fig. 12. Average radial spectra for the three test areas, calculated by averaging Fourier amplitudes within concentric bands of width 0.2 rad/km centered about the origin.

regions are transformed into the wave number domain, where they can be interpreted readily in terms of their spectral properties and compared with the spectral properties of neighboring regions. The following discussion demonstrates this approach.

As before, we let $\mathbf{s} = (x, y)$ and $\mathbf{k} = (k_x, k_y)$ represent horizontal coordinates in the space and Fourier domains, respectively, and make use of the convolution operation for functions of two variables, defined by

$$u(\mathbf{s}) * v(\mathbf{s}) = \int_{-\infty}^{\infty} \int_{-\infty}^{\infty} u(\mathbf{s}_0) v(\mathbf{s} - \mathbf{s}_0) dx_0 dy_0 \quad (8)$$

The wave number coordinates k_x and k_y are related to wavelengths λ_x and λ_y by $k_x = 2\pi/\lambda_x$ and $k_y = 2\pi/\lambda_y$. The Fourier transform (equation (3)) and the convolution operation (equation (8)) are related to each other by the convolution theorem:

$$\mathcal{F}[u(\mathbf{s}) * v(\mathbf{s})] = \mathcal{F}[u(\mathbf{s})] \cdot \mathcal{F}[v(\mathbf{s})] \quad (9)$$

The vertical attraction at a point $(x, y, 0)$ due to a density distribution $\rho(x, y, z)$ is given by

$$g_z(\mathbf{s}) = G \int_{z_0} \rho(\mathbf{s}, z_0) * f(\mathbf{s}, z_0) dz_0 \quad (10a)$$

where G is the gravitational constant and

$$f(\mathbf{s}, z) = \frac{\partial}{\partial z} \frac{1}{(|\mathbf{s}|^2 + z^2)^{1/2}} \quad (10b)$$

Applying the Fourier transform to both sides of equation (10a) and using relation (9) yields

$$\mathcal{F}[g_z(\mathbf{s})] = G \int_{z_0} \mathcal{F}[\rho(\mathbf{s}, z_0)] \cdot \mathcal{F}[f(\mathbf{s}, z_0)] dz_0 \quad (11)$$

The Fourier transform of $f(\mathbf{s}, z_0)$ is given by

$$\mathcal{F}[f(\mathbf{s}, z_0)] = 2\pi e^{-z_0|\mathbf{k}|} \quad (12)$$

where $|\mathbf{k}| = (k_x^2 + k_y^2)^{1/2}$ [Blakely, 1977], and substituting (12) into (11) yields

$$\mathcal{F}[g_z(\mathbf{s})] = 2\pi G \int_{z_0} \exp(-|\mathbf{k}|z_0) \cdot \mathcal{F}[\rho(\mathbf{s}, z_0)] dz_0 \quad (13)$$

Thus the Fourier transform of a gravitational anomaly represents an exponentially weighted sum of Fourier transforms of the density distribution. Equation (13) demonstrates that contributions from deep-crustal sources, especially SWL contributions, will be subdued in the space domain relative to shallower but otherwise similar sources. Moreover, deep sources will be dominated by their shallower counterparts in the Fourier domain and will be significant only near $|\mathbf{k}| = 0$. Unfortunately, this is the region of the Fourier domain that is most poorly defined.

In the following example, three areas (Figure 11) with dissimilar anomaly patterns were selected from the isostatic residual gravity map for comparison of spectral properties. Each area has dimensions of about 1000 by 1000 km. Area A, covering the Basin and Range province, is characterized by SWL anomalies produced by lows over sediment-filled basins and by broad low-amplitude anomalies of uncertain origin. Area B, which encompasses the Laramide ranges of Wyoming and neighboring states, is dominated by longer-wavelength, high-amplitude anomalies related to upthrust crustal sections in the Laramide ranges and by lows over the intervening sedimentary basins floored by downwarped crustal sections. Area C in the midcontinent region includes high-amplitude anomalies over the MGH, the step in base level across the MGH, and a fabric of SWL anomalies of diverse trends.

The gravity data from each area were Fourier-transformed, amplitudes were calculated for each Fourier value, and the resulting grids were smoothed into overlapping cells, 10 points on each side, to improve statistical resolution [Claerbout, 1976]. The x axis was considered positive to the right (approximately east) and the y axis positive upward (approximately north). Only the amplitude spectrum $A(\mathbf{k}) = |\mathcal{F}[g_z(\mathbf{s})]|$ was considered for each area. The color plots along the left side of Plate 4 show $\ln A^2(\mathbf{k})$ for each area out to $k_x = k_y = \pm\pi/10$ rad/km ($\lambda_x = \lambda_y = \pm 20$ km). The contour interval is 1.0; because these maps are logarithms of squared amplitudes, each contour represents an amplitude 0.61 times less than the amplitude represented by the next highest contour. Thus most of the power in the isostatic residual data is condensed very near the origin of the Fourier domain.

All three spectra are perfectly symmetrical through their respective origins, as expected for Fourier transforms of real data. Each spectrum also has a high degree of radial symmetry. Equation (13) shows that any deviation from radial symmetry must be caused by horizontal variations in the density distribution $\rho(x, y, z)$. To emphasize these deviations, we have found it useful to normalize each amplitude spectrum by dividing by its respective radially symmetric part:

$$A_0(\mathbf{k}) = A(\mathbf{k})/R(|\mathbf{k}|) \quad (14)$$

where

$$R(|\mathbf{k}|) = \int_0^{2\pi} A(\mathbf{k}) d\theta \quad (15a)$$

$$|\mathbf{k}| = (k_x^2 + k_y^2)^{1/2} \quad (15b)$$

and

$$\theta = \tan^{-1}(k_y/k_x) \quad (15c)$$

Figure 12 shows $\ln R^2(|\mathbf{k}|)$ for each area. These radial spectra were calculated by averaging the Fourier amplitudes within bands of width 0.02 rad/km concentric about the origin. The normalized amplitude spectra were then calculated in accordance with equation (14) and the results are shown along the right side of Plate 4.

Figure 12 demonstrates that the rate of attenuation with increasing $|\mathbf{k}|$ is greater in areas B and C than in area A. As shown by equation (13), the rate of attenuation with increasing $|\mathbf{k}|$ is largely controlled by the depth of sources but can also be influenced by the nature of the density distribution $\rho(x, y, z)$. An area with dimensionally large gravity sources will be deficient in SWL amplitudes relative to an area with dimensionally small sources. Without independent knowledge about the density distributions, we conclude that area A is distinguishable from areas B and C by generally shallower sources, dimensionally smaller sources, or both. It is not surprising that many of the sources within area A are relatively shallow, because crystalline basement is widely exposed at the surface in this region, whereas the important sources within area C lie beneath several kilometers of sedimentary material. Moreover, the gravity sources within area A are likely to be dimensionally smaller than those within areas B and C because of their different tectonic histories. Area A includes the Basin and Range province, which has developed largely by extensional tectonic processes. Area B is dominated by anomalies over the Laramide ranges, major uplifts of basement rocks due to compressional events. Area C includes the MGH, caused by mafic material related to failed rifting. The tectonic history of area A probably has produced a more complex and shorter wavelength distribution of upper crustal densities than the tectonic histories of areas B and C.

Maxima in $A_0(\mathbf{k})$ (Plate 4) indicate specific wavelengths in $\rho(\mathbf{s})$ of relatively high energy [Bracewell, 1965]. Consider, for example, a sinusoidal density distribution between depths z_1 and z_2 , with corrugations trending at an angle ϕ , measured counterclockwise from the positive x axis, and with a wavelength λ , measured normal to the corrugations:

$$\rho(\mathbf{s}) = \cos \left[\frac{2\pi}{\lambda} (-x \sin \phi + y \cos \phi) \right] \quad (16)$$

Then,

$$\mathcal{F}[\rho(\mathbf{s})] = 2\pi^2 [\delta(k_x - k_\alpha, k_y - k_\beta) + \delta(k_x + k_\alpha, k_y + k_\beta)] \quad (17)$$

where $k_\alpha = (-2\pi/\lambda) \sin \phi$ and $k_\beta = (2\pi/\lambda) \cos \phi$. It is clear from equations (13) and (14) that $A(\mathbf{k})$ will have precisely the same form as equation (17):

$$A(\mathbf{k}) = C [\delta(k_x - k_\alpha, k_y - k_\beta) + \delta(k_x + k_\alpha, k_y + k_\beta)] \quad (18)$$

where C is a constant. Thus, by locating the coordinates $\mathbf{k} = (k_\alpha, k_\beta)$ of the maxima in $A_0(\mathbf{k})$, the trend ϕ and wavelength λ of dominant components of $\rho(\mathbf{s})$ can be calculated according to

$$\tan \phi = -k_\alpha/k_\beta \quad (19)$$

and

$$\lambda = \frac{2\pi}{(k_\alpha^2 + k_\beta^2)^{1/2}} \quad (20)$$

Large, linear highs in $A_0(\mathbf{k})$ appear along both the k_x and k_y axes in all three areas (Plate 4) because the discrete Fourier analysis assumes that $\rho(\mathbf{s})$ is periodic in both the x and y

directions. The highs along $k_x = 0$ and $k_y = 0$ reflect our attempt to force nonperiodic data through an inherently periodic procedure; they do not necessarily reflect dominant north-south or east-west trends of anomalies within areas A, B, and C, other than those caused by the edges of our rectangular map area.

Plate 1 shows that area A is dominated by SWL north to northwest trending anomalies corresponding to the general geologic and topographic expression of the Basin and Range province. We expect, therefore, that the spectral analysis will show this dominant pattern. In Plate 4, area A has a conspicuous maximum at $\mathbf{k} = (0.130, 0.040)$. Applying equations (19) and (20), we conclude that this maximum reflects a dominant sinusoidal component within $\rho(\mathbf{s})$, with a wavelength of 46 km and a trend of 107° . Area A also has a maximum at $\mathbf{k} = (0.240, 0.100)$, which corresponds to $\lambda = 24$ km and $\phi = 113^\circ$. These maxima in the Fourier domain manifest the pattern of anomalies in the Basin and Range province.

In area B, maxima exist at $\mathbf{k} = (0.310, -0.125)$, $(0.310, 0.305)$, and $(0.05, 0.025)$, corresponding to $\phi = 68^\circ$, 135° , and 116° , and $\lambda = 19, 14,$ and 112 km, respectively. The second two maxima form part of a ridge in the Fourier domain that trends through the origin at an angle of approximately 45° from the k_x axis. This ridge indicates that structures of various wavelengths exist in $\rho(\mathbf{s})$ with approximately northwest trends. Many of the anomalies over the Laramide ranges have trends with similar directions (Plate 1). The maxima in $A_0(\mathbf{k})$ may manifest the preexisting structural fabric of the basement, as well as the compressional events that produced the uplifted Laramide ranges.

In area C, maxima exist at $\mathbf{k} = (0.060, -0.040)$ and $(0.150, -0.130)$, which correspond to sinusoids with $\phi = 56^\circ$ and 49° and to $\lambda = 87$ and 32 km, respectively. The MGH has a northeast trend similar to these along most of its length through area C. The maxima in $A_0(\mathbf{k})$ probably reflect density patterns in the upper crust related to the rifting processes that created the MGH.

CONCLUSIONS

1. Isostatic residual gravity maps of continental areas are easy to construct and experiment with, once the gravity and topographic data are available in digital form. Editing and correcting these digital data sets remains the most difficult part of the job.

2. For the purpose of displaying anomalies, trends, and patterns caused by features of geologic interest, the choice of isostatic model is less important than the application of an isostatic correction of some sort. Most reasonable compensation models produce an isostatic regional that approximates the effect of upward continuation of the topography as if it were a potential field, to some height related to the depth of compensation. (A constant multiplier must also be applied to convert elevations to milliGals.) The differences are of less interest than the overall patterns if the goal is to highlight shallow density contrasts of geologic importance.

3. It is almost impossible to determine from gravity data alone whether an individual isostatic residual anomaly has a source that is in local isostatic balance or imbalance. In the absence of information to the contrary, the most productive approach for interpreting such anomalies is probably to assume that they are completely compensated and to use as much relevant geologic and geophysical data to construct a density model of the source bodies. If the bodies are not in

isostatic balance, then their imbalance should become apparent in the modeling process if enough additional geologic and geophysical constraints are available.

4. Many short-wavelength isostatic residual anomalies can be attributed to geologic features mapped at the surface or in the shallow subsurface. The causes of such anomalies less than several hundred kilometers wide have been tentatively classified into a small number of geologic-tectonic categories. This should aid in the interpretation of highs and lows in regions where the source bodies are not exposed at the surface. Most high anomalies whose sources are known can be attributed to mafic rocks in rift settings or to accreted or upthrust dense, commonly mafic, material. Most lows can be explained in terms of sedimentary deposits, generally in convergent tectonic settings, to felsic igneous rocks, both extrusive as in calderas and intrusive as in batholiths, and to downwarped crustal sections. Many anomalies are caused by features of Precambrian age or are suspected to be caused by reactivations of such features by later tectonic events.

5. Anomalies at least several hundred kilometers wide on the isostatic residual map compare well with similar anomalies on free air gravity maps, and the broadest anomalies appear on satellite-derived gravity maps. Several intermediate-wavelength anomalies appear to correlate with geologic features exposed at the surface; these anomalies are hypothesized to be caused by density contrasts that lie, at least in part, in the crust. All the anomalies in the isostatic residual gravity field of the conterminous United States with wavelengths of several hundred to several thousand kilometers can be explained by isostatically balanced and geologically reasonable density contrasts confined to the upper 200 km of crust and mantle. This explanation does not preclude the possibility of deeper sources for these anomalies, but it does indicate that an appeal to deeper sources may not be necessary in all cases.

6. Spectral analysis of subareas on the isostatic residual gravity map that appear to the eye to have quite different anomaly patterns yields amplitude spectra that highlight the differences between these subareas in more objective and quantitative ways. Specifically, spectral analysis helps to identify dominant trends and their wavelengths in the distribution of crustal densities. This approach may help in comparisons of terranes judged to be similar or dissimilar on other grounds.

Acknowledgments. We wish to thank James Case, Andrew Griscom, Carl Wentworth, and Mark Zoback for their longstanding encouragement and interest in the preparation of these maps. The results have been much improved by their comments and by the criticisms of Warren Hamilton, David Harwood, Walter Mooney, David Ponce, Ray Wells, and Mary Lou Zoback. Case and Griscom also gave us much help in the construction of Table 2, and many others freely shared their ideas and insights into the meanings of isostatic anomalies. Thanks are also due Scott Smithson and an anonymous reviewer for their thoughtful criticisms.

REFERENCES

- Aiken, C. L. V., Analysis of the gravity anomalies in Arizona, Ph.D. thesis, 127 pp., Univ. of Ariz., Tucson, 1976.
- Aiken, C. L. V., J. C. Lysonski, J. S. Sumner, and W. R. Hahman, Sr., A series of 1:250,000 complete residual Bouguer gravity anomaly maps of Arizona, *Ariz. Geol. Soc. Dig.*, 13, 31–38, 1981.
- Aiken, O. W., G. R. Keller, and W. J. Hinze, Geologic significance of surface gravity measurements in the vicinity of the Illinois deep drill holes, *J. Geophys. Res.*, 88, 7307–7314, 1983.
- Airy, G. B., On the computation of the effect of the attraction of the mountain-masses, as disturbing the apparent astronomical latitude of stations in geodetic surveys, *Philos. Trans. R. Soc. London*, 145, 101–104, 1855.
- Aldrich, M. J., Jr., M. E. Ander, and A. W. Laughlin, Geological and geophysical signatures of the Jemez Lineament: A reactivated Precambrian structure, in *International Basement Tectonics*, vol. 4, pp. 77–85, Basement Tectonics Committee, Inc., Denver, Colo., 1984.
- Allenby, R. J., and C. C. Schnetzer, United States crustal thickness, *Tectonophysics*, 93, 13–31, 1983.
- Anderson, E. R., M. L. Zoback, and G. A. Thompson, Implications of selected subsurface data on the structural form and evolution of some basins in the northern Basin and Range province, Nevada and Utah, *Geol. Soc. Am. Bull.*, 94, 1055–1072, 1983.
- Arvidson, R. E., E. A. Guinness, J. W. Strebeck, G. F. Davies, and K. J. Schulz, Image processing applied to gravity and topography data covering the continental U.S., *Eos Trans. AGU*, 63, 261–265, 1982.
- Bally, A. W., Basins and subsidence—A summary, in *Dynamics of Plate Interiors, Geodyn. Ser.*, vol. 1, edited by A. W. Bally, P. L. Bender, T. R. McGetchin, and R. I. Walcott, pp. 5–20, AGU, Washington, D. C., 1980.
- Banks, R. J., R. L. Parker, and S. P. Huestis, Isostatic compensation on a continental scale: Local versus regional mechanisms, *Geophys. J. R. Astron. Soc.*, 51, 431–452, 1977.
- Barnes, V. E., F. Romberg, and W. A. Anderson, Geology and geophysics of Blanco and Gillespie counties, Texas, in *Cambrian Field Trip—Llano Area, March 19–20, 1954*, edited by V. E. Barnes and W. C. Bell, pp. 78–90, San Angelo Geological Society, San Angelo, Tex., 1954.
- Bayley, R. W., and W. R. Muehlberger, Basement rock map of the United States, scale 1:2,500,000, U.S. Geol. Surv., Reston, Va., 1968.
- Best, D. M., W. H. Geddes, and J. S. Watkins, Gravity investigation of the depth of source of the Piedmont gravity gradient in Davidson County, North Carolina, *Geol. Soc. Am. Bull.*, 84, 1213–1216, 1973.
- Beyer, L. A., Offshore southern California, Interpretation of the Gravity Map of California and its Continental Margin, edited by H. W. Oliver, *Bull. Calif. Div. Mines Geol.*, 205, 8–15, 1980.
- Bickford, M. E., K. L. Harrower, W. J. Hoppe, B. K., Nelson, R. L. Nusbaum, and J. J. Thomas, Rb-Sr and U-Pb geochronology and distribution of rock types in the Precambrian basement of Missouri and Kansas, *Geol. Soc. Am. Bull.*, 92, 323–341, 1981a.
- Bickford, M. E., J. R. Sides, and R. L. Cullers, Chemical evolution of magmas in the Proterozoic terrane of the St. Francois Mountains, southeastern Missouri, 1, Field, petrographic, and major element data, *J. Geophys. Res.*, 86, 10,365–10,386, 1981b.
- Bird, P., Laramide crustal thickening event in the Rocky Mountain foreland and Great Plains, *Tectonics*, 3, 741–758, 1984.
- Blake, M. C., Jr., R. H. Campbell, T. W. Dibblee, Jr., D. G. Howell, T. H. Nilsen, W. R. Normark, J. C. Vedder, and E. A. Silver, Neogene basin formation in relation to plate-tectonic evolution of the San Andreas fault system, California, *Am. Assoc. Pet. Geol. Bull.*, 62, 344–372, 1978.
- Blakely, R. J., Documentation for subroutine REDUC3, an algorithm for the linear filtering of gridded magnetic data, *U.S. Geol. Surv. Open File Rep. 77-784*, 27 pp., 1977.
- Blakely, R. J., and R. W. Simpson, Locating edges of source bodies from magnetic or gravity anomalies, *Geophysics*, 51, 1494–1498, 1986.
- Blakely, R. J., R. C. Jachens, R. W. Simpson, and R. W. Couch, Tectonic setting of the southern Cascade Range as interpreted from its magnetic and gravity fields, *Geol. Soc. Am. Bull.*, 96, 43–48, 1985.
- Bott, M. H. P., and S. B. Smithson, Gravity investigations of subsurface shape and mass distributions of granite batholiths, *Geol. Soc. Am. Bull.*, 78, 859–878, 1967.
- Bowie, W., Effect of topography and isostatic compensation upon the intensity of gravity (second paper), *U.S. Coast Geod. Surv. Spec. Publ.*, 12, 28 pp., 1912.
- Bowie, W., Investigations of gravity and isostasy, *U.S. Coast Geod. Surv. Spec. Publ.*, 40, 196 pp., 1917.
- Bowie, W., Isostatic investigations and data for gravity stations in the United States established since 1915, *U.S. Coast Geod. Surv. Spec. Publ.*, 99, 91 pp., 1924.
- Bowin, C., Depth of principal mass anomalies contributing to the earth's geoidal undulations and gravity anomalies, *Mar. Geol.*, 7, 61–100, 1983.
- Bowin, C., W. Warsi, and J. Milligan, Free-air gravity anomaly map of the world, scale approximately 1:22,000,000, *Map Chart Ser. MC-45*, Geol. Soc. of Am., Boulder, Colo., 1982.
- Brace, W. F., and D. L. Kohlstedt, Limits on lithospheric stress im-

- posed by laboratory experiments, *J. Geophys. Res.*, **85**, 6248–6252, 1980.
- Bracewell, R., *The Fourier Transform and Its Applications*, 381 pp., McGraw-Hill, New York, 1965.
- Brewer, J. A., L. D. Brown, D. Steiner, J. E. Oliver, S. Kaufman, and R. E. Denison, Proterozoic basin in the southern midcontinent of the United States revealed by COCORP deep seismic reflection profiling, *Geology*, **9**, 569–575, 1981.
- Brown, L., L. Jenson, J. Oliver, S. Kaufman, and D. Steiner, Rift structure beneath the Michigan basin from COCORP profiling, *Geology*, **10**, 645–649, 1982.
- Burke, K., Intracontinental rifts and aulacogens, in *Continental Tectonics*, edited by B. C. Burchfiel, J. E. Oliver, and L. T. Silver, pp. 42–49, National Academy of Sciences, Washington, D. C., 1980.
- Byerly, P. E., Interpretations of gravity data from the central Coast Ranges and San Joaquin valley, California, *Geol. Soc. Am. Bull.*, **77**, 83–94, 1966.
- Cady, J. W., Magnetic and gravity anomalies in the Great Valley and western Sierra Nevada metamorphic belt, California, *Spec. Pap. Geol. Soc. Am.*, **168**, 56 pp., 1975.
- Camfield, P. A., and D. I. Gough, A possible Proterozoic plate boundary in North America, *Can. J. Earth Sci.*, **14**, 1229–1238, 1977.
- Case, J. E., and H. R. Joesting, Regional geophysical investigations of the central Colorado plateau, *U.S. Geol. Surv. Prof. Pap.*, **736**, 31 pp., 1972.
- Case, J. E., and W. R. Keefer, Regional gravity survey of the Wind River basin, Wyoming, *U.S. Geol. Surv. Prof. Pap.*, **550-C**, C120–C128, 1966.
- Cathles, L. M., III, *The Viscosity of the Earth's Mantle*, 386 pp., Princeton University Press, Princeton, N. J., 1975.
- Chapman, M. E., and J. H. Bodine, Considerations of the indirect effect in marine gravity modeling, *J. Geophys. Res.*, **84**, 3889–3896, 1979.
- Chapman, M. E., and M. Talwani, Comparison of gravimetric geoids with GEOS 3 altimetric geoid, *J. Geophys. Res.*, **84**, 3803–3816, 1979.
- Chapman, R. H., and A. Griscom, Coast Ranges, Interpretation of the Gravity Map of California and Its Continental Margin, edited by H. W. Oliver, *Bull. Calif. Div. Mines Geol.*, **205**, 24–27, 1980.
- Chase, C. G., and T. H. Gilmer, Precambrian plate tectonics: The mid-continent gravity high, *Earth Planet. Sci. Lett.*, **21**, 70–78, 1973.
- Claerbout, J. F., *Fundamentals of Geophysical Data Processing with Applications to Petroleum Prospecting*, 274 pp., McGraw-Hill, New York, 1976.
- Clayton, R. W., and R. P. Comer, A tomographic analysis of mantle heterogeneities from body wave travel times, *Eos Trans. AGU*, **64**, 776, 1983.
- Condie, K. C., Plate-tectonic model for Proterozoic continental accretion in the southwestern United States, *Geology*, **10**, 37–42, 1982.
- Cook, F. A., and J. E. Oliver, The late Precambrian–early Paleozoic continental edge in the Appalachian orogen, *Am. J. Sci.*, **281**, 993–1008, 1981.
- Cook, F. A., D. S. Albaugh, L. D. Brown, S. Kaufman, J. E. Oliver, and R. D. Hatcher, Jr., Thin-skinned tectonics in the crystalline southern Appalachians; COCORP seismic-reflection profiling of the Blue Ridge and Piedmont, *Geology*, **7**, 563–567, 1979.
- Cook, F. A., L. D. Brown, S. Kaufman, J. E. Oliver, and T. A. Petersen, COCORP seismic profiling of the Appalachian orogen beneath the Coastal Plain of Georgia, *Geol. Soc. Am. Bull.*, **92**, 738–748, 1981.
- Cordell, L., Regional geophysical setting of the Rio Grande rift, *Geol. Soc. Am. Bull.*, **89**, 1073–1090, 1978.
- Cordell, L., Extension in the Rio Grande rift, *J. Geophys. Res.*, **87**, 8561–8569, 1982.
- Craddock, C., E. C. Thiel, and B. Gross, A gravity investigation of the Precambrian of southeastern Minnesota and western Wisconsin, *J. Geophys. Res.*, **68**, 6015–6032, 1963.
- Dainty, A. M., and J. E. Frazier, Bouguer gravity in northeastern Georgia: A buried suture, a surface suture, and granites, *Geol. Soc. Am. Bull.*, **95**, 1168–1175, 1984.
- Daly, R. A., *Strength and Structure of the Earth*, 434 pp., Prentice-Hall, Englewood Cliffs, N. J., 1940.
- Decker, E. R., and S. B. Smithson, Heat flow and gravity interpretation across the Rio Grande rift in southern New Mexico and west Texas, *J. Geophys. Res.*, **80**, 2542–2552, 1975.
- Dehlinger, P., R. W. Couch, and M. Gemperle, Continental and oceanic structure from the Oregon Coast westward across the Juan de Fuca ridge, *Can. J. Earth Sci.*, **5**, 1079–1090, 1968.
- Denison, R. E., E. G. Lidiak, M. E. Bickford, and E. B. Kisvarsanyi, Geology and geochronology of Precambrian rocks in the central interior region of the United States, *U.S. Geol. Surv. Prof. Pap.*, **1241-C**, C1–C20, 1984.
- DeRito, R. F., F. A. Cozzarelli, and D. S. Hodge, Mechanism of subsidence of ancient cratonic rift basins, *Tectonophysics*, **94**, 141–168, 1983.
- Dorman, L. M., and B. T. R. Lewis, Experimental isostasy, 1, Theory of the earth's isostatic response to a concentrated load, *J. Geophys. Res.*, **75**, 3357–3365, 1970.
- Dorman, L. M., and B. T. R. Lewis, Experimental isostasy, 3, Inversion of the isostatic Green function and lateral density changes, *J. Geophys. Res.*, **77**, 3068–3077, 1972.
- Dutch, S. I., Proterozoic structural provinces in the north-central United States, *Geology*, **11**, 478–481, 1983.
- Dutton, C. E., On some of the greater problems of physical geology, *Bull. Philos. Soc. Wash.*, **11**, 51–64, 1889. (Reprinted in *J. Wash. Acad. Sci.*, **15**, 359–369, 1925.)
- Dziewonski, A. M., Mapping the lower mantle: Determination of lateral heterogeneity in *P* velocity up to degree and order 6, *J. Geophys. Res.*, **89**, 5929–5952, 1984.
- Eaton, G. P., R. L. Christiansen, H. M. Iyer, A. M. Pitt, D. R. Mabey, H. R. Blank, Jr., I. Zietz, and M. E. Gettings, Magma beneath Yellowstone National Park, *Science*, **188**, 787–796, 1975.
- Gerhard, L. C., S. B. Anderson, J. A. Lefever, and C. G. Carlson, Geological development, origin and energy mineral resources of Williston basin, North Dakota, *Am. Assoc. Pet. Geol. Bull.*, **66**, 989–1020, 1982.
- Gettings, M. E., H. R. Blank, W. D. Mooney, and J. H. Healy, Crustal structure of southwestern Saudi Arabia, *J. Geophys. Res.*, **91**, 6491–6512, 1986.
- Gibb, R. A., A geological interpretation of the Bouguer anomalies adjacent to the Churchill-Superior boundary in northern Manitoba, *Can. J. Earth Sci.*, **5**, 439–453, 1968.
- Gibb, R. A., and M. D. Thomas, Gravity signature of fossil plate boundaries in the Canadian Shield, *Nature*, **262**, 199–200, 1976.
- Gibb, R. A., and R. I. Walcott, A Precambrian suture in the Canadian Shield, *Earth Planet. Sci. Lett.*, **10**, 417–422, 1971.
- Gibb, R. A., M. D. Thomas, P. L. LaPointe, and M. Mukhopadhyay, Geophysics of proposed Proterozoic sutures in Canada, *Precambrian Res.*, **19**, 349–384, 1983.
- Gilbert, G. K., Interpretation of anomalies of gravity, *U.S. Geol. Surv. Prof. Pap.*, **85-C**, 27–37, 1913.
- Gilbert, M. C., Timing and chemistry of igneous events associated with the southern Oklahoma aulacogen, *Tectonophysics*, **94**, 439–455, 1983.
- Godson, R. H., and D. M. Scheibe, Description of magnetic tape containing conterminous U.S. gravity data in gridded format, *Rep. PB82-254798*, magnetic tape with description, 5 pp., Natl. Tech. Inf. Serv., Springfield, Va., 1982.
- Graaff-Hunter, J. de, Notices Scientifique, Report of study group no. 8, Reduction of observed gravity, *Bull. Geod., New Ser.*, **50**, 1–16, 1958.
- Green, A. G., G. L. Cumming, and D. Cedarwell, Extension of the Superior-Churchill boundary zone into southern Canada, *Can. J. Earth Sci.*, **16**, 1691–1701, 1979.
- Green, A. G., Z. Hajnal, and W. Weber, An evolutionary model of the western Churchill province and western margin of the Superior province in Canada and the north-central United States, *Tectonophysics*, **116**, 281–322, 1985.
- Green, J. C., Geologic and geochemical evidence for the nature and development of the Middle Proterozoic (Keweenaw) midcontinent rift of North America, *Tectonophysics*, **94**, 413–437, 1983.
- Griscom, A., Tectonic significance of the Bouguer gravity field of the Appalachian System, *Spec. Pap. Geol. Soc. Am.*, **73**, 163–164, 1963.
- Griscom, A., and H. W. Oliver, Isostatic gravity highs along the west side of the Sierra Nevada and the Peninsular Ranges batholiths, California (abstract), *Eos Trans. AGU*, **61**, 1126, 1980.
- Guinness, E. A., R. E. Arvidson, J. W. Strebeck, K. J. Schulz, G. F. Davies, and C. E. Leff, Identification of a Precambrian rift through Missouri by digital image processing of geophysical and geological data, *J. Geophys. Res.*, **87**, 8529–8545, 1982.
- Hamilton, W., Plate-tectonic mechanism of Laramide deformation, *Contrib. Geol.*, **19**(2), 87–92, 1981.
- Harris, L. D., and K. C. Bayer, Sequential development of the Appa-

- lachian orogen above a master decollement—A hypothesis, *Geology*, 7, 568–572, 1979.
- Harrison, J. C., R. E. von Huene, and C. E. Corbato, Bouguer gravity anomalies and magnetic anomalies off the coast of southern California, *J. Geophys. Res.*, 71, 4921–4941, 1966.
- Haworth, R. T., D. L. Daniels, H. Williams, and I. Zietz, Bouguer gravity anomaly map of the Appalachian orogen. Scale 1:1,000,000, *Map 3*, Mem. Univ. of Newfoundland, St. Johns, 1980.
- Hayford, J. F., and W. Bowie, The effect of topography and isostatic compensation upon the intensity of gravity, *U.S. Coast Geod. Surv. Spec. Publ.*, 10, 132 pp., 1912.
- Heiskanen, W. A., and H. Moritz, *Physical Geodesy*, 364 pp., W. H. Freeman, New York, 1967.
- Hildenbrand, T. G., FFTFIL: A filtering program based on two-dimensional Fourier analysis of geophysical data, *U.S. Geol. Surv. Open File Rep.*, 83–237, 61 pp., 1983.
- Hildenbrand, T. G., Rift structure of the northern Mississippi embayment from the analysis of gravity and magnetic data, *J. Geophys. Res.*, 90, 12,607–12,622, 1985.
- Hildenbrand, T. G., M. F. Kane, and J. D. Hendricks, Magnetic basement in the upper Mississippi Embayment region—A preliminary report, Investigations of the New Madrid, Mississippi Earthquake Region, edited by F. A. McKeown and L. C. Pakiser, *U.S. Geol. Surv. Prof. Pap.*, 1236-E, 39–53, 1982.
- Hinze, W. J., A gravity investigation of the Baraboo syncline region, *J. Geol.*, 67, 417–446, 1959.
- Hinze, W. J., R. L. Kellogg, and N. W. O'Hara, Geophysical studies of basement geology of southern peninsula of Michigan, *Am. Assoc. Pet. Geol. Bull.*, 59, 1562–1584, 1975.
- Hinze, W. J., J. W. Bradley, and A. R. Brown, Gravimeter survey of the Michigan basin deep borehole, *J. Geophys. Res.*, 83, 5864–5868, 1978.
- Hoffman, P., J. F. Dewey, and K. Burke, Aulacogens and their genetic relationship to geosynclines, with a Proterozoic example from the Great Slave Lake, Canada, *Spec. Publ. Soc. Econ. Paleontol. Mineral.*, 19, 38–55, 1974.
- Horton, J. W., Jr., I. Zietz, and T. L. Neathery, Truncation of the Appalachian Piedmont beneath the Coastal Plain of Alabama: Evidence from new magnetic data, *Geology*, 12, 51–55, 1984.
- Hurich, C. A., and S. B. Smithson, Gravity interpretation of the southern Wind River Mountains, Wyoming, *Geophysics*, 47, 1550–1561, 1982.
- Hutchinson, D. R., J. A. Grow, K. D. Klitgord, and B. A. Swift, Deep structure and evolution of the Carolina trough, *Studies in Continental Margin Geology*, edited by J. S. Watkins and C. L. Drake, *Mem. Am. Assoc. Pet. Geol.*, 34, 129–152, 1982.
- Hutchinson, D. R., J. A. Grow, and K. D. Klitgord, Crustal structure beneath the southern Appalachians: Nonuniqueness of gravity modeling, *Geology*, 11, 611–615, 1983.
- Jachens, R. C., and A. Griscom, Three-dimensional geometry of the Gorda plate beneath northern California, *J. Geophys. Res.*, 88, 9375–9392, 1983.
- Jachens, R. C., and A. Griscom, An isostatic residual gravity map of California—A residual map for interpretation of anomalies from intracrustal sources, in *The Utility of Regional Gravity and Magnetic Anomaly Maps*, edited by W. J. Hinze, pp. 347–360, Society of Exploration Geophysicists, Tulsa, Okla., 1985.
- Jachens, R. C., C. G. Barnes, and M. M. Donato, Subsurface configuration of the Orleans fault: Implications for deformation in the western Klamath Mountains, California, *Geol. Soc. Am. Bull.*, 97, 388–395, 1986a.
- Jachens, R. C., R. W. Simpson, R. W. Saltus, and R. J. Blakely, Isostatic residual gravity anomaly map of the United States (exclusive of Alaska and Hawaii), map on clear film, scale 1:2,500,000, Geophys. Data Cent., Natl. Oceanic Atmos. Admin., Boulder, Colo., 1986b.
- Johnson, R. A., K. E. Karlstrom, S. B. Smithson, and R. S. Houston, Gravity profiles across the Cheyenne Belt, a Precambrian crustal suture in southeastern Wyoming, *J. Geodyn.*, 1, 445–472, 1984.
- Jordan, T. M., Composition and development of the continental tectosphere, *Nature*, 274, 544–548, 1978.
- Kahle, H., S. Mueller, E. Klingele, R. Egloff, and E. Kissling, Recent dynamics, crustal structure and gravity in the Alps, in *Earth Rheology, Isostasy and Eustasy*, edited by N. Mörner, pp. 377–388, John Wiley, New York, 1980.
- Kane, M. F., and R. H. Godson, Features of a pair of long-wavelength (>250 km) and short-wavelength (<250 km) Bouguer gravity maps of the United States, in *The Utility of Regional Gravity and Magnetic Anomaly Maps*, edited by W. J. Hinze, pp. 46–61, Society of Exploration Geophysicists, Tulsa, Okla., 1985.
- Kane, M. F., D. R. Mabey, and R. L. Brace, A gravity and magnetic investigation of the Long Valley caldera, Mono County, California, *J. Geophys. Res.*, 81, 754–762, 1976.
- Kane, M. F., T. G. Hildenbrand, and J. D. Hendricks, Model for the tectonic evolution of the Mississippi embayment and its contemporary seismicity, *Geology*, 9, 563–568, 1981a.
- Kane, M. F., M. W. Webring, and B. K. Bhattacharyya, A preliminary analysis of gravity and aeromagnetic surveys of the Timber Mountain area, southern Nevada, *U.S. Geol. Surv. Open File Rep.*, 81-189, 40 pp., 1981b.
- Kärki, P., L. Kivioja, and W. A. Heiskanen, Topographic-isostatic reduction maps for the world for the Hayford zones 18-1, Airy-Heiskanen system, $T = 30$ km, *Publ. 35*, 23 pp., Isostatic Inst. of the Int. Assoc. of Geod., Helsinki, 1961.
- Karlstrom, K. E., and R. S. Houston, The Cheyenne belt: Analysis of a Proterozoic suture in southern Wyoming, *Precambrian Res.*, 25, 415–446, 1984.
- Karner, G. D., and A. B. Watts, On isostasy at Atlantic-type continental margins, *J. Geophys. Res.*, 87, 2923–2948, 1982.
- Karner, G. D., and A. B. Watts, Gravity anomalies and flexure of the lithosphere at mountain ranges, *J. Geophys. Res.*, 88, 10,449–10,477, 1983.
- Kaula, W. M., Global gravity and mantle convection, *Tectonophysics*, 13, 341–359, 1972.
- Keller, G. R., J. M. Hills, and R. Djeddi, A regional geological and geophysical study of the Delaware Basin, New Mexico and West Texas, *Field Conf. Guideb. N. M. Geol. Soc.*, 31, 105–111, 1980.
- Keller, G. R., A. E. Bland, and J. K. Greenberg, Evidence for a major late Precambrian tectonic event (rifting?) in the eastern midcontinent region, United States, *Tectonics*, 1, 213–223, 1982a.
- Keller, G. R., R. A. Smith, W. J. Hinze, and C. L. V. Aiken, Geologic significance of regional gravity and magnetic anomaly maps of Trans-Pecos, Texas, paper presented at the 52nd International Meeting and Exposition, Soc. of Explor. Geophys., Dallas, Tex., 1982b.
- King, E. R., and I. Zietz, Aeromagnetic study of the midcontinent gravity high of the central United States, *Geol. Soc. Am. Bull.*, 82, 2187–2208, 1971.
- King, P. B., *The Evolution of North America*, 197 pp., Princeton University Press, Princeton, N. J., 1977.
- King, P. B., and H. M. Beikman, Geologic map of the United States, scale 1:2,500,000, U.S. Geol. Surv., Reston, Va., 1974.
- Klasner, J. S., and E. R. King, Precambrian basement geology of North and South Dakota, *Can. J. Earth Sci.*, in press, 1986.
- Klasner, J. S., E. R. King, and W. J. Jones, Geologic and gravity interpretation of gravity and magnetic data for northern Michigan and Wisconsin, in *The Utility of Regional Gravity and Magnetic Anomaly Maps*, edited by W. J. Hinze, pp. 267–286, Society of Exploration Geophysicists, Tulsa, Okla., 1985.
- Klitgord, K. D., and P. Popenoe, Florida: A Jurassic transform plate boundary, *J. Geophys. Res.*, 89, 7753–7772, 1984.
- Kovach, R. L., C. R. Allen, and F. Press, Geophysical investigations in the Colorado delta region, *J. Geophys. Res.*, 67, 2845–2871, 1962.
- LaFehr, T. R., Gravity, isostasy, and crustal structure in the southern Cascade Range, *J. Geophys. Res.*, 70, 5581–5597, 1965.
- LaFehr, T. R., Gravity in the eastern Klamath Mountains, California, *Geol. Soc. Am. Bull.*, 77, 1177–1190, 1966.
- Lambeck, K., Estimate of stress differences in the crust from isostatic considerations, *J. Geophys. Res.*, 85, 6397–6402, 1980.
- Lerch, F. J., S. M. Klosko, R. E. Laubscher, and C. A. Wagner, Gravity model improvement using GEOS 3 (GEM 9 and 10), *J. Geophys. Res.*, 84, 3897–3920, 1979.
- Lewis, B. T. R., and L. M. Dorman, Experimental isostasy, 2, An isostatic model for the U.S.A. derived from gravity and topographic data, *J. Geophys. Res.*, 75, 3367–3386, 1970.
- Lidiak, E. G., W. J. Hinze, G. R. Keller, J. E. Reed, L. W. Braille, and R. W. Johnson, Geologic significance of regional gravity and magnetic anomalies in the east-central midcontinent, in *The Utility of Regional Gravity and Magnetic Anomaly Maps*, edited by W. J. Hinze, pp. 287–307, Society of Exploration Geophysicists, Tulsa, Okla., 1985.
- Lillie, R. J., Tectonically buried continent/ocean boundary, Ouachita Mountains, Arkansas, *Geology*, 13, 18–21, 1985.
- Lillie, R. J., K. D. Nelson, B. de Voogd, J. A. Brewer, J. E. Oliver, L.

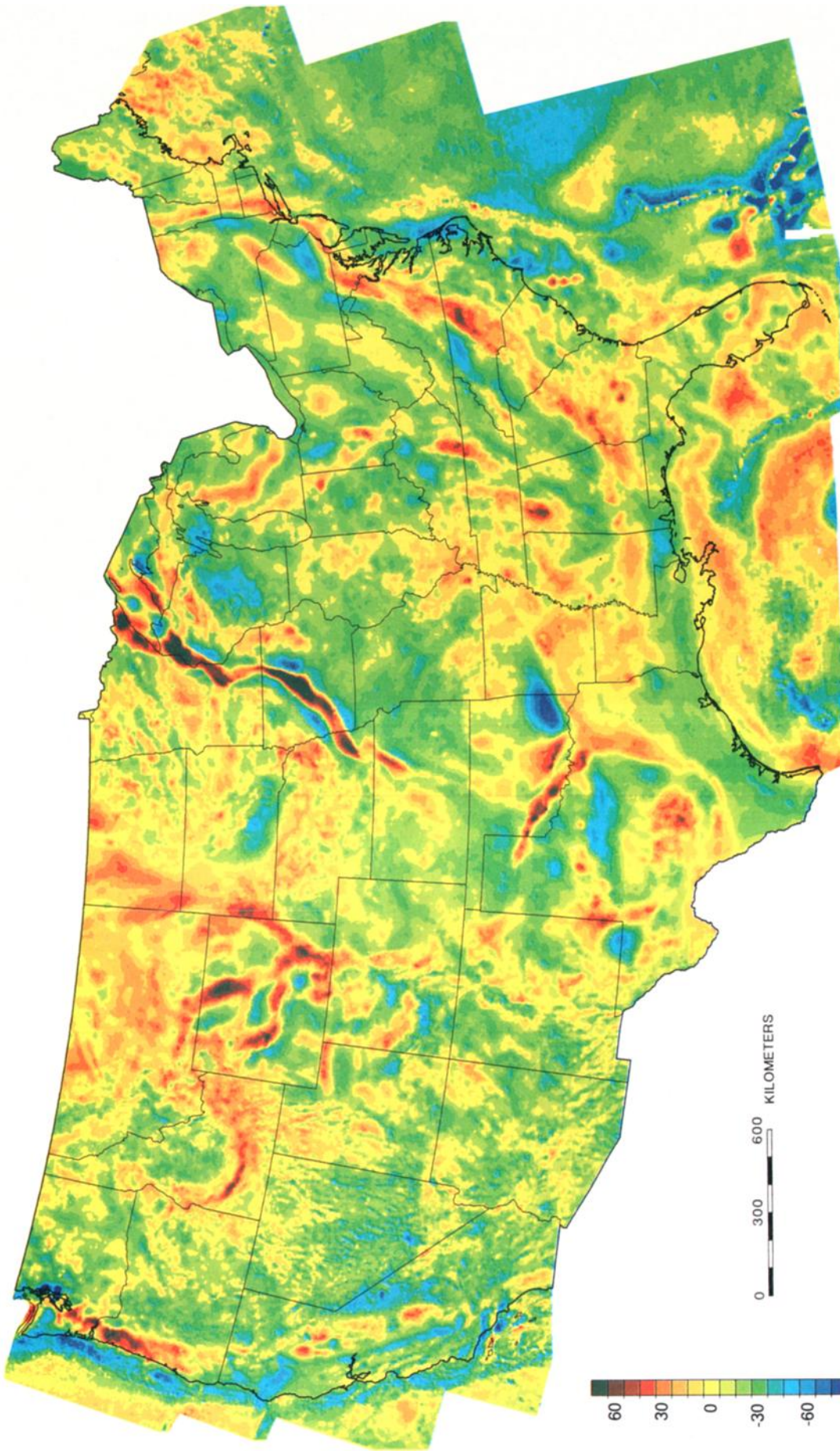
- D. Brown, S. Kaufman, and G. W. Viele, Crustal structure of Ouachita Mountains, Arkansas: A model based on integration of COCORP reflection profiles and regional geophysical data, *Am. Assoc. Pet. Geol. Bull.*, 67, 907-931, 1983.
- Lynn, H. B., L. D. Hale, and G. A. Thompson, Seismic reflections from the basal contacts of batholiths, *J. Geophys. Res.*, 86, 10,633-10,638, 1981.
- Lyon, P. L., Geophysical background of Arkoma basin tectonics, *Tulsa Geol. Soc. Dig.*, 29, 94-104, 1961.
- Mabey, D. R., Relation between Bouguer gravity anomalies and regional topography in Nevada and the Eastern Snake River Plain, Idaho, *U.S. Geol. Surv. Prof. Pap.*, 550-B, B108-B110, 1966.
- Mabey, D. R., Interpretation of a gravity profile across the western Snake River plain, Idaho, *Geology*, 4, 53-55, 1976.
- McGinnis, L. D., Tectonics and gravity field in the continental interior, *J. Geophys. Res.*, 75, 317-331, 1970.
- McGinnis, L. D., M. G. Wolf, J. J. Kohsmann, and C. P. Ervin, Regional free air gravity anomalies and tectonic observations in the United States, *J. Geophys. Res.*, 84, 591-601, 1979.
- McKenzie, D., Some remarks on the development of sedimentary basins, *Earth Planet. Sci. Lett.*, 40, 25-32, 1978.
- McNutt, M., Implications of regional gravity for state of stress in the earth's crust and upper mantle, *J. Geophys. Res.*, 85, 6377-6396, 1980.
- McNutt, M., Influence of plate subduction on isostatic compensation in northern California, *Tectonics*, 2, 399-415, 1983.
- Mitchell, B. J., and M. Landisman, Interpretation of a crustal section across Oklahoma, *Geol. Soc. Am. Bull.*, 81, 2647-2656, 1970.
- Mörner, N., *Earth Rheology, Isostasy and Eustasy*, 599 pp., John Wiley, New York, 1980.
- Neidell, N. S., A statistical study of isostasy, *Geophys. Prospect.*, 11, 164-175, 1963.
- Nelson, K. D., R. J. Lillie, B. de Voogd, J. A. Brewer, J. E. Oliver, S. Kaufman, L. Brown, and G. W. Viele, COCORP seismic reflection profiling in the Ouachita Mountains of western Arkansas: Geometry and geologic interpretation, *Tectonics*, 1, 413-430, 1982.
- Nicholas, R. L., and R. A. Rozendal, Subsurface positive elements within Ouachita foldbelt in Texas and their relation to Paleozoic cratonic margin, *Am. Assoc. Pet. Geol. Bull.*, 59, 193-216, 1975.
- Ocola, L. C., and R. P. Meyer, Central North American rift system, 1, Structure of the axial zone from seismic and gravimetric data, *J. Geophys. Res.*, 78, 5173-5194, 1973.
- O'Hara, N. W., and P. L. Lyons, New map updates gravity data, *Geotimes*, 28, 22-27, 1983.
- Oliver, H. W., Gravity and magnetic investigations of the Sierra Nevada batholith, California, *Geol. Soc. Am. Bull.*, 88, 445-461, 1977.
- Oliver, H. W., and D. R. Mabey, Anomalous gravity field in east-central California, *Geol. Soc. Am. Bull.*, 74, 1293-1298, 1963.
- Parker, R. L., The rapid calculation of potential anomalies, *Geophys. J. R. Astron. Soc.*, 31, 447-455, 1972.
- Pindell, J. L., Alleghenian reconstruction and subsequent evolution of the Gulf of Mexico, Bahamas, and Proto-Caribbean, *Tectonics*, 4, 1-39, 1985.
- Plouff, D., and L. C. Pakiser, Gravity study of the San Juan Mountains, Colorado, *U.S. Geol. Surv. Prof. Pap.*, 800-B, B183-B190, 1972.
- Powell, B. N., and J. F. Fischer (Eds.), Plutonic igneous geology of the Wichita magmatic province, Oklahoma, *10th Annu. Meet. Field Trip Guideb.* 2, 35 pp., South Cent. Sect., Geol. Soc. of Am., Manhattan, Kan., 1976.
- Powell, B. N., and D. W. Phelps, Igneous cumulates of the Wichita province and their tectonic implications, *Geology*, 5, 52-56, 1977.
- Powell, B. N., M. C. Gilbert, and J. F. Fischer, Lithostratigraphic classification of basement rocks of the Wichita province, Oklahoma, *Geol. Soc. Am. Bull.*, Part 1, 91, 509-514, 1980.
- Pratt, J. H., On the attraction of the Himalaya Mountains, and of the elevated regions beyond them upon the plumb-line in India, *Philos. Trans. R. Soc. London*, 145, 53-100, 1855.
- Pruatt, M. A., Geophysical interpretations, Plutonic Igneous Geology of the Wichita Magmatic Province, Oklahoma, edited by B. N. Powell and J. F. Fischer, *10th Annu. Meet. Field Trip Guideb.* 2, pp. 4-7, South Cent. Sect., Geol. Soc. of Am., Manhattan, Kan., 1976.
- Putnam, G. R., Relative determinations of gravity with half-second pendulums, and other pendulum investigations, report of the Superintendent of the U.S. Coast and Geodetic Survey showing the progress of the work during the fiscal year ending with June 1894, part II, Appendix 1, pp. 9-50, U.S. Coast Geod. Surv., Rockville, Md., 1894.
- Putnam, G. R., Results of a transcontinental series of gravity measurements, *Bull. Philos. Soc. Wash.*, 13, 31-60, 1895.
- Rabinowitz, P. D., The boundary between oceanic and continental crust in the western North Atlantic, in *The Geology of Continental Margins*, edited by C. A. Burk and C. L. Drake, pp. 67-84, Springer-Verlag, New York, 1974.
- Rabinowitz, P. D., and J. L. LaBrecque, The isostatic gravity anomaly: Key to the evolution of the ocean-continent boundary at passive continental margins, *Earth Planet. Sci. Lett.*, 35, 145-150, 1977.
- Ramberg, I. B., F. A. Cook, and S. B. Smithson, Structure of the Rio Grande rift in southern New Mexico and west Texas based on gravity interpretation, *Geol. Soc. Am. Bull.*, 89, 107-123, 1978.
- Richards, M. A., and B. H. Hager, Geoid anomalies in a dynamic earth, *J. Geophys. Res.*, 89, 5987-6002, 1984.
- Rodgers, J., *The Tectonics of the Appalachians*, Wiley-Interscience, New York, 1970.
- Saltus, R. W., A description of colored gravity and terrain maps of the southwestern cordillera, *U.S. Geol. Surv. Open File Rep.*, 84-95, 8 pp., 1984.
- Shanmugam, G., and G. G. Lash, Analogous tectonic evolution of the Ordovician foredeeps, southern and central Appalachians, *Geology*, 10, 562-566, 1982.
- Simmons, G., Gravity survey and geological interpretation, northern New York, *Geol. Soc. Am. Bull.*, 75, 81-98, 1964.
- Simpson, R. W., T. H. Hildenbrand, R. H. Godson, and M. F. Kane, A description of colored gravity and terrain maps for the conterminous United States, shown on 35mm slides, *U.S. Geol. Surv. Open File Rep.*, 82-477, 7 pp., 1982.
- Simpson, R. W., R. C. Jachens, and R. J. Blakely, AIRYROOT: A Fortran program for calculating the gravitational attraction of an Airy isostatic root out to 166.7 km, *U.S. Geol. Surv. Open File Rep.*, 83-883, 66 pp., 1983a.
- Simpson, R. W., R. W. Saltus, R. C. Jachens, and R. H. Godson, A description of colored isostatic gravity maps and a topographic map of the conterminous United States available as 35mm slides, *U.S. Geol. Surv. Open File Rep.*, 83-884, 16 pp., 1983b.
- Simpson, R. W., R. C. Jachens, R. W. Saltus, and R. J. Blakely, Isostatic residual gravity, topographic, and first-vertical-derivative gravity maps of the conterminous United States, scale 1:7,500,000, *U.S. Geol. Surv. Geophys. Invest. Map*, GP-975, 1986.
- Sleep, N. H., and L. L. Sloss, The Michigan Basin, in *Dynamics of Plate Interiors*, *Geodyn. Ser.*, vol. 1, edited by A. W. Bally, P. L. Bender, T. R. McGetchin, and R. I. Walcott, pp. 93-98, AGU, Washington, D. C., 1980.
- Smithson, S. B., J. A. Brewer, S. Kaufman, J. E. Oliver, and C. A. Hurich, Structure of the Laramide Wind River uplift, Wyoming, from COCORP deep reflection data and from gravity data, *J. Geophys. Res.*, 84, 5955-5972, 1979.
- Snavely, P. D., Jr., H. C. Wagner, and D. L. Lander, Interpretation of the Cenozoic geologic history, central Oregon continental margin: Cross-section summary, *Geol. Soc. Am. Bull.*, 91, 143-146, 1980.
- Society of Exploration Geophysicists, Gravity anomaly map of the United States (exclusive of Alaska and Hawaii), scale 1:2,500,000, Tulsa, Okla., 1982.
- Sparlin, M. A., L. W. Braile, and R. B. Smith, Crustal structure of the eastern Snake River plain determined from ray trace modeling of seismic refraction data, *J. Geophys. Res.*, 87, 2619-2633, 1982.
- Sprenke, K. F., and E. R. Kanasewich, Gravity modelling in western Canada, paper presented at the 52nd International Meeting and Exposition, Soc. of Explor. Geophys., Dallas, Tex., 1982.
- Stanley, W. D., Tectonic study of Cascade Range and Columbia Plateau in Washington State based upon magnetotelluric soundings, *J. Geophys. Res.*, 89, 4447-4460, 1984.
- Stephenson, R., and K. Lambeck, Isostatic response of the lithosphere with in-plane stress: application to central Australia, *J. Geophys. Res.*, 90, 8581-8588, 1985.
- Strange, W. E., and G. P. Woollard, The use of geologic and geophysical parameters in the evaluation, interpolation, and prediction of gravity, *Hawaii Inst. Geophys. Rep.*, HIG 64-17, IV-1-IV-42, 1964.
- Stuart, D. J., Gravity study of crustal structure in western Washington, *U.S. Geol. Surv. Prof. Pap.*, 424-C, C273-C276, 1961.
- Sumner, J. R., Geophysical investigation of the structural framework of the Newark-Gettysburg Triassic basin, Pennsylvania, *Geol. Soc. Am. Bull.*, 88, 935-942, 1977.

- Suppe, J., Structural interpretation of the southern part of the northern Coast Ranges and Sacramento Valley, California: Summary, *Geol. Soc. Am. Bull.*, 90, 327-330, 1979.
- Thomas, J. J., R. D. Shuster, and M. E. Bickford, A terrane of 1,350- to 1,400-m.y.-old silicic volcanic and plutonic rocks in the buried Proterozoic of the mid-continent and in the Wet Mountains, Colorado, *Geol. Soc. Am. Bull.*, 95, 1150-1157, 1984.
- Thomas, M. D., Tectonic significance of paired gravity anomalies in the southern and central Appalachians, *Mem. Geol. Soc. Am.*, 158, 113-124, 1983.
- Thompson, G. A., Gravity measurements between Hazen and Austin, Nevada: A study of basin-Range structure, *J. Geophys. Res.*, 64, 217-229, 1959.
- Thompson, G. A., and D. B. Burke, Regional geophysics of the Basin and Range province, *Annu. Rev. Earth Planet. Sci.*, 2, 213-238, 1974.
- Van Schmus, W. R., and M. E. Bickford, Proterozoic chronology and evolution of the midcontinent region, North America, in *Precambrian Plate Tectonics*, edited by A. Kröner, pp. 261-296, Elsevier Science, New York, 1981.
- Vening Meinesz, F. A., Tables fondamentales pour la réduction isostatique régionale, *Bull. Geod.*, 63, 711-776, 1939.
- Wehr, F., and L. Glover, III, Stratigraphy and tectonics of the Virginia-North Carolina Blue Ridge: Evolution of a late Proterozoic-early Paleozoic hinge zone, *Geol. Soc. Am. Bull.*, 96, 285-295, 1985.
- Williams, H., Tectonic lithofacies map of the Appalachian orogen, scale 1:1,000,000, *Map 1*, Mem. Univ. of Newfoundland, St. John's, 1978.
- Woodhouse, J. H., and A. M. Dziewonski, Mapping the upper mantle: Three-dimensional modeling of earth structure by inversion of seismic waveforms, *J. Geophys. Res.*, 89, 5953-5986, 1984.
- Woollard, G. P., An interpretation of gravity-anomalies in terms of local and regional geologic structures, *Eos Trans. AGU*, 17, 63-74, 1936.
- Woollard, G. P., The relation of gravity anomalies to surface elevation, crustal structure, and geology, *Res. Rep. 62-9*, 356 pp., Geophys. Polar Res. Cent., Univ. of Wis., Madison, 1962.
- Woollard, G. P., Regional isostatic relations in the United States, in *The Earth Beneath the Continents*, *Geophys. Monog. Ser.*, vol. 10, edited by J. S. Steinhardt, and T. J. Smith, pp. 557-594, AGU, Washington, D. C., 1966.
- Woollard, G. P., The interrelationship of the crust, the upper mantle, and isostatic gravity anomalies in the United States, in *The Crust and Upper Mantle of the Pacific Area*, *Geophys. Monogr. Ser.*, vol. 12, edited by L. Knopoff, C. L. Drake, and P. J. Hart, pp. 312-341, AGU, Washington, D. C., 1968.
- Woollard, G. P., Regional variations in gravity, in *The Nature of the Solid Earth*, edited by E. C. Robertson, pp. 463-505, McGraw-Hill, New York, 1972.
- Woollard, G. P., Regional changes in gravity and their relation to crustal parameters, in *Volcanoes and Tectonosphere*, 370 pp., edited by A. Hitoshi and S. Iizuka, Tokai University Press, Tokyo, 1976.
- Zietz, I., Composite magnetic anomaly map of the United States, Part A, Conterminous United States, scale 1:2,500,000, *U.S. Geol. Surv. Geophys. Invest. Map GP-954A*, 1982.
- Zoback, M. L., and A. H. Lachenbruch, Upper mantle structure beneath the western U.S., *Geol. Soc. Am. Abstr. Programs*, 16, 705, 1984.

R. J. Blakely, R. C. Jachens, and R. W. Simpson, U.S. Geological Survey, 345 Middlefield Road, MS 977, Menlo Park, CA 94025.

R. W. Saltus, U.S. Geological Survey, MS 964 Denver Federal Center, Box 25046, Denver, CO 80225.

(Received September 18, 1985;
revised March 5, 1986;
accepted March 6, 1986.)



MILLIGALS

ISOSTATIC RESIDUAL GRAVITY

Plate 1 [Simpson *et al.*]. Isostatic residual gravity map of the conterminous United States, prepared using an Airy-Heiskanen local compensation model with the following parameters: density of surface load, 2.67 g/cm³; density contrast at depth, 0.35 g/cm³; and depth to bottom of root for sea level elevations, 30 km. Accuracy of most onland gravity values is estimated to be better than 5 mGal; accuracies of offshore values are mostly better than 10–20 mGal. Certain offshore anomalies less than about 40 km wide, occurring in areas where bottom depths are changing rapidly, result because the Bouguer correction was applied to gridded offshore free air data, using the 5- by 5-min bathymetric data set to infer depths. These small anomalies, which can be in error by as much as 40 mGal, appear as small spots of color on the map at this scale.

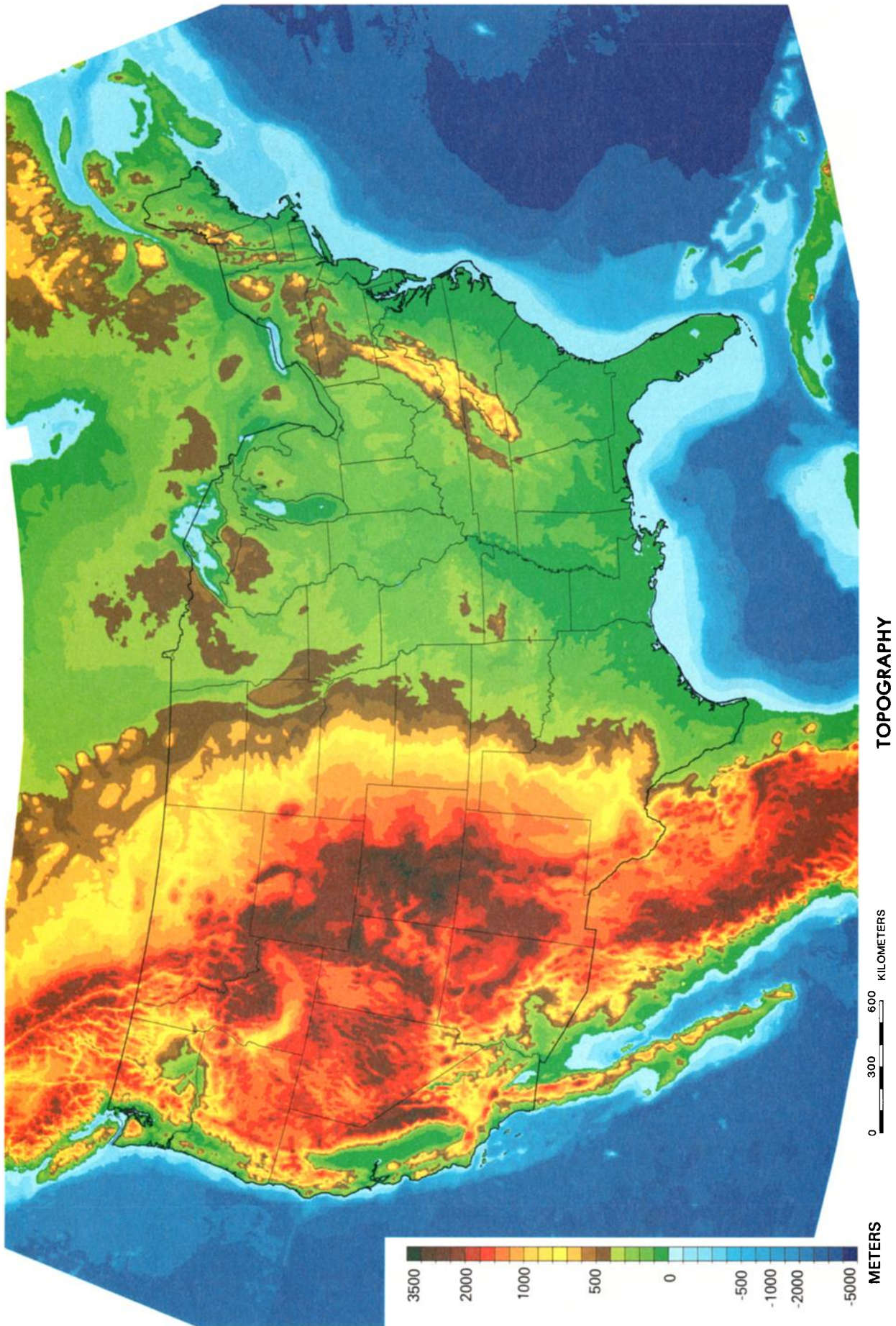
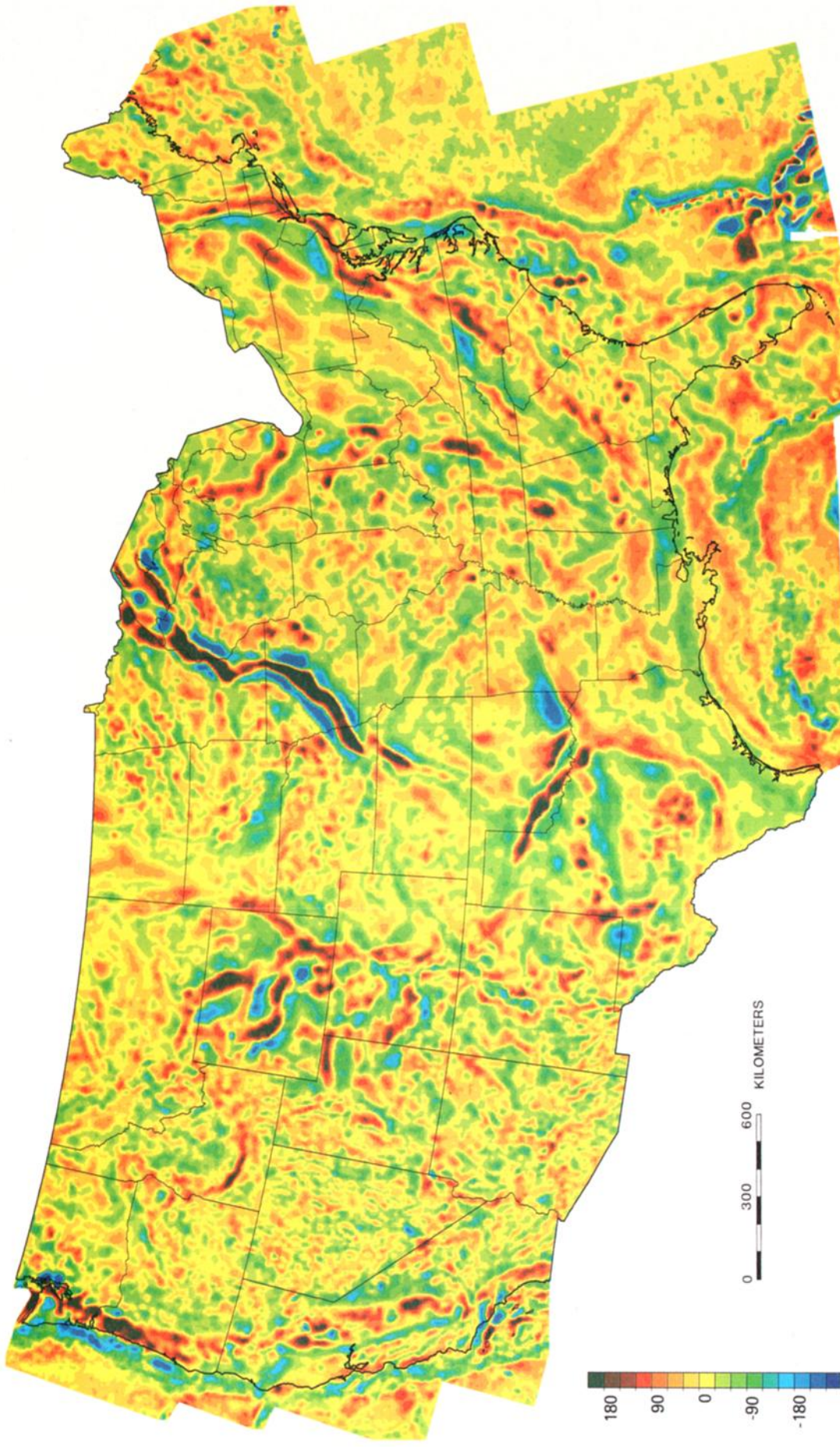


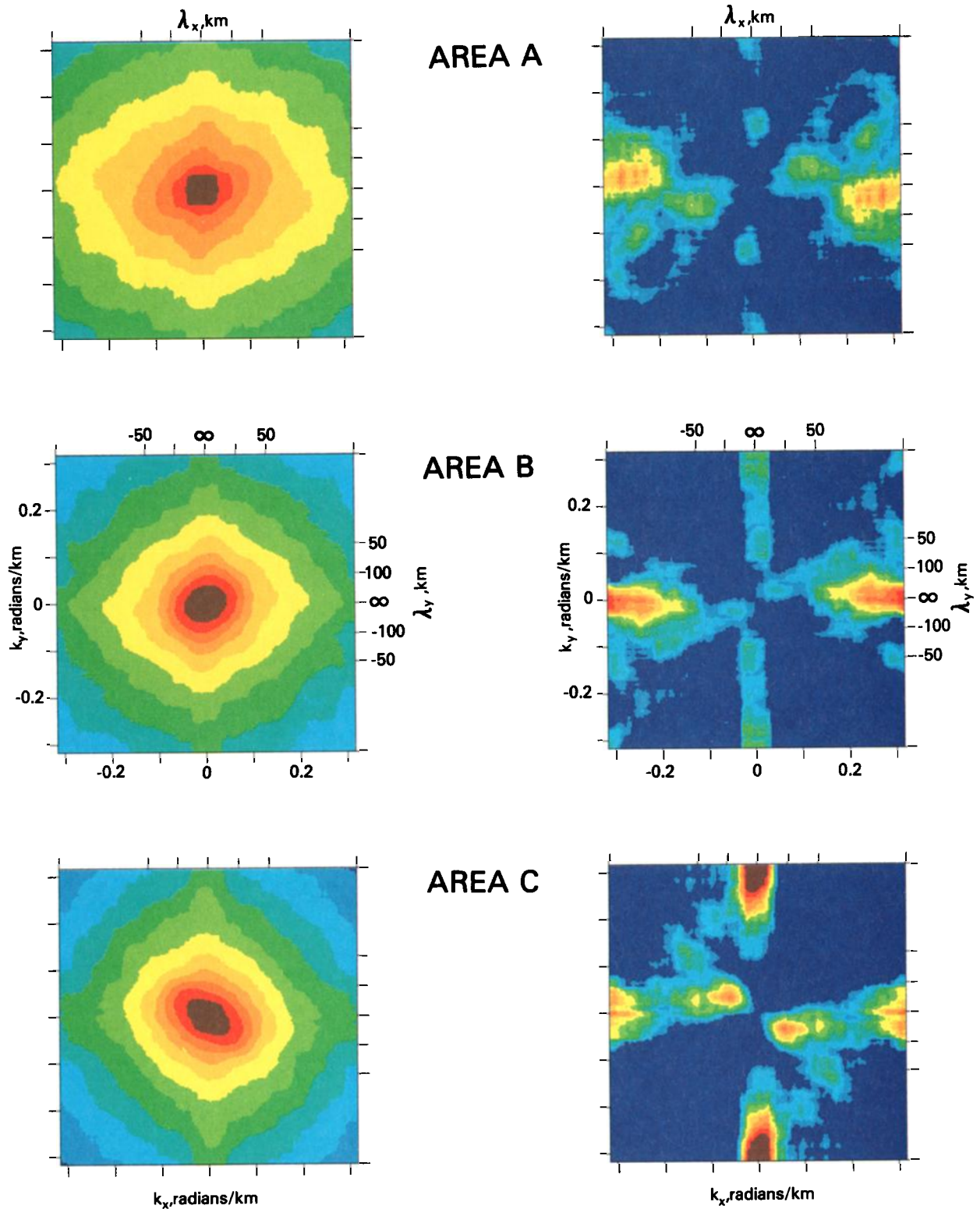
Plate 2 [Simpson et al.]. Topographic map prepared from 5- by 5-min averaged topographic and bathymetric data. Color scale is not linear.



PSEUDOGAMMAS

FIRST VERTICAL DERIVATIVE OF ISOSTATIC RESIDUAL GRAVITY

Plate 3 [Simpson *et al.*]. First vertical derivative of the isostatic residual map shown in Plate 1. This is a pseudomagnetic map, as explained in the text, and units are in milliGals per kilometer multiplied by a factor of 149.9. This factor gives a scale in nanoteslas for the total magnetic field that would be observed at the pole if material of density contrast 0.1 g/cm³ were to be replaced by magnetic material of magnetization 0.001 emu/cm³.



AMPLITUDE SPECTRA

Plate 4 [Simpson et al.]. Amplitude spectra for the three test areas (Figure 12). (Left) Smoothed, two-dimensional Fourier transforms of areas A, B, and C. Color levels represent logarithms of squared amplitudes, with a contour interval of 1. (Right) Normalized amplitude spectra, calculated by dividing the amplitude spectra by average radial spectra (Figure 12). Color levels represent logarithms of squared amplitudes, with a contour interval of 0.1. Levels less than 0 not shown.